OROGRAPHIC FORCING IN LARGE-SCALE GCM EXPERIMENTS

S. Tibaldi

European Centre for Medium
Range Weather Forecasts,
England

ABSTRACT

This lecture intends to review, with no pretence of completeness, some of the numerical experiments reported in the literature on the importance of mountain representation in general circulation experiments.

It is planned to create a more realistic global orography for operational use at ECMWF. It is hoped that this review, in addition to being of general interest to those attending the September Seminars, will provide a "literature background" to the work of assessing the impact of this more realistic orography on the behaviour of the operational model and on the quality of the forecasts.

1. INTRODUCTION

The importance of the corrugations of the lower boundary of the Earth's atmosphere in determining the characteristics of the general circulation has been recognized long ago (e.g. Charney and Eliassen, 1949, Bolin, 1950, Gambo, 1956).

Following Lorenz (1967) into his classification of the principal features of the circulation into four categories, as follows:

(1) *Features which appear when the variables are averaged with respect to time and longitude.* These are typified by the familiar trade winds. A time average may mean an average over all time, or over all years at a particular time of the year. Some writers prefer to restrict the term "general circulation" to features in this category, and it is these features which, directly or indirectly, will receive the major attention in this monograph.

(2) *Features in addition to those of the first category which appear when the variables are averaged with respect to time alone.* These are typified by the Asiatic summer and winter monsoons. Most writers include these as features of the general circulation.

(3) *Features in addition to those of the first category which appear when the variables are averaged with respect to longitude alone.* These are typified by the familiar fluctuations of the zonal index. Studies of these features are ordinarily regarded as general-circulation studies by those engaged in them.

(4) *Features in addition to those of the first three categories which appear when the variables are not averaged.* These are typified by migratory cyclones. Many of these features are ordinarily regarded as secondary circulations; some of their over-all statistical properties are frequently considered to be characteristic of the general circulation.

It is possible to show that mountains have an important (if not primary) influence on all four categories of general circulation features listed above.

Starting from the last point, they, for example, strongly participate in determining the areas of preferred cyclogenesis on the globe (Manabe and Terpstra, 1974). For what point 3) is concerned, they play a fundamental role in generating blocking (Egger, 1979). About point 2), it has ben shown that they determine to a great extent the pattern of standing waves in the westerlies.

The influence of mountains in the first category is less obvious. It is, in fact, possible in principle to try to reproduce the observed zonally-averaged climatology by modelling an equivalent "billiard-ball" planet and tuning the various "knobs" of the model atmosphere until it reproduces as close as possible the "target" climatology.

This is, in fact, what for some time has been done with GCM's. It is, therefore, not surprising if, in some examples, the straightforward introduction of "an orography" (or, for that matter, the improvement of a particularly well-behaved orography towards reality) in an already tuned GCM did not produce the expected improvements in representing some climatological features. The inherent non-linearity of GCM's does not, in fact, guarantee such an improvement.

2. MOUNTAINS AND POTENTIAL VORTICITY

One of the simplest ways to interpret the dynamical influence of mountains on the large scale flow is through the conservation of some form of Potential Vorticity.

This, for adiabatic and frictionless motion takes the form of

$$\frac{D}{Dt}\left\{\frac{\zeta + f}{\frac{\partial p}{\partial \theta}}\right\} = 0 \qquad 2.1$$

Due to vortex shrinking and stretching, the parcels of fluid that flow over a mountain ridge have to deflect from a straight trajectory.

Simple arguments (see e.g. Holton, 1972) lead to the conclusion that, while the influence of the ridge on an easterly flow will remain confined to the ridge region, (Fig. 2.2) westerly flow over a barrier will cause generation of Rossby-type planetary waves, (Fig. 2.1). These waves transport momentum and feed on the energy of the mean motion (they convert K.E. of the basic state into K.E. of the standing eddy), but need not, in principle, to transport heat.

A very simple model fluid that exhibits the property of conserving a "Potential Vorticity" is defined by the shallow-water equations, for which the conservation becomes:

$$\frac{D}{Dt}\left\{\frac{\zeta + f}{(h - H)}\right\} = 0 \qquad 2.2$$

where h is the height of the fluid and H is the height of the lower boundary.

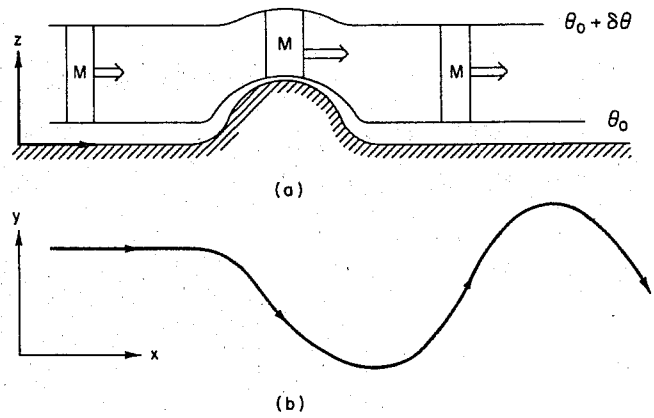

Fig. 2.1

Westerly flow over a topographic barrier: (a) the depth of a column as a function of x, (b) the trajectory of a parcel in the x, y plane. (After Holton, 1972)

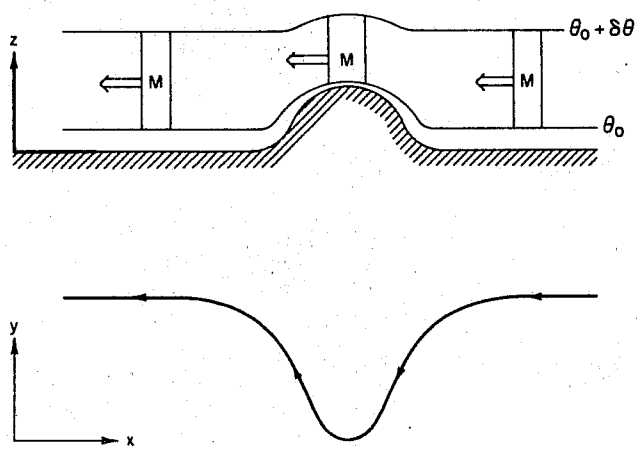

Fig. 2.2

Easterly flow over a topographic barrier. (After Holton, 1972)

Following Kasahara (1966) we will now briefly inspect the flow of a "shallow", inviscid, incompressible, homogeneous fluid in a periodic channel where a hemispheric obstacle has been placed. We will here consider five cases:

Case A : westerly flow, f-plane

Case B : westerly flow, β-plane

Case C : easterly flow, β-plane

Case D : fast westerly, β-plane

Cade E : slow westerly, β-plane

The flow is started from the initial conditions:

$$u = \bar{u}(\text{const}) \qquad h = \bar{h} = h_o - \frac{\bar{u}}{g} \int_o^y f(y)\, dy$$

$$v = 0$$

The wind field and the mass field are not, therefore, balanced initially over the mountain region

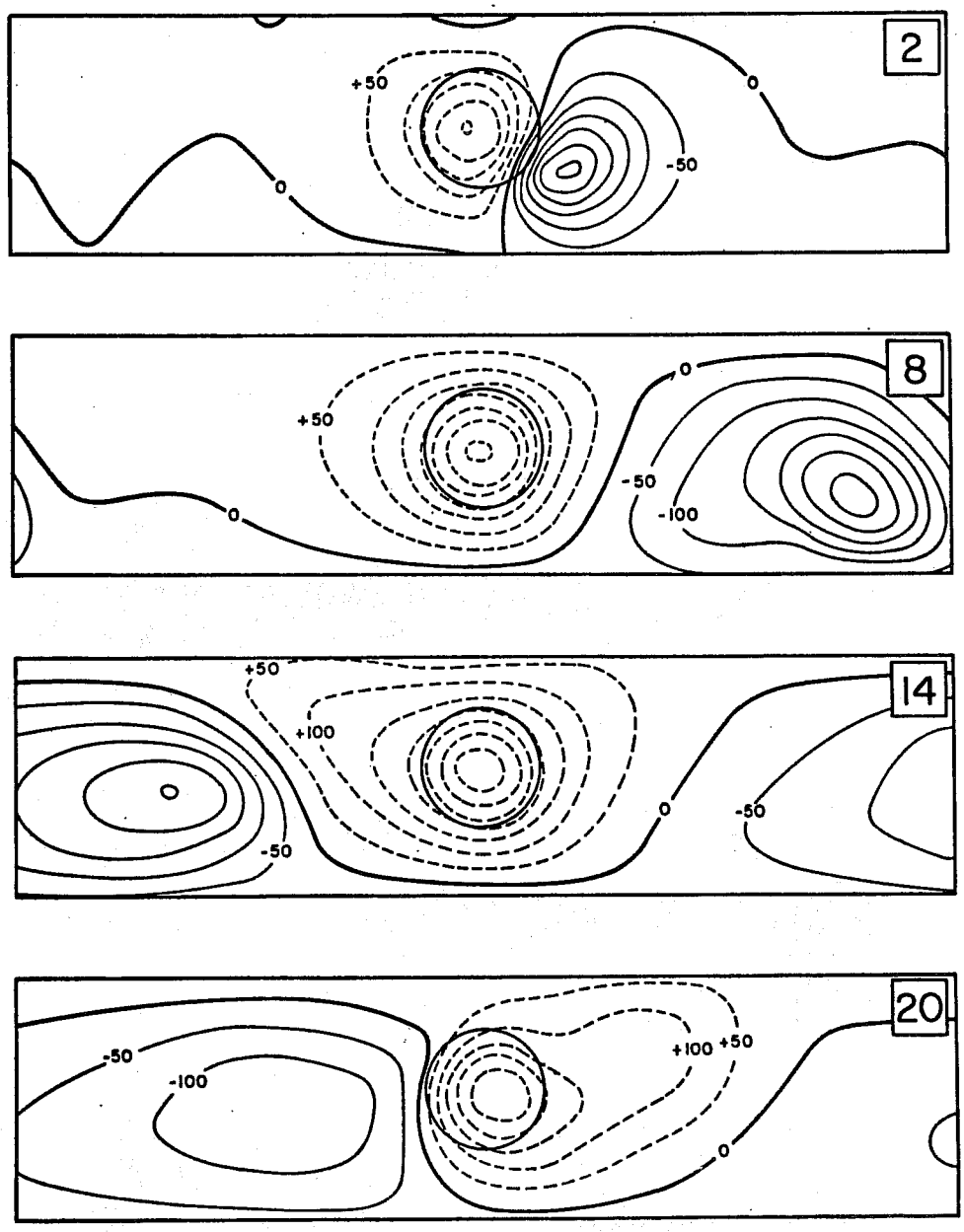

Constant f, U = 20 m/s

Evolution of height deviation field of Case A. Time, in days, is given in the upper right corner of each chart. Circular obstacle is indicated by the circle. Contours are drawn for every 50-m interval. (After Kasahara, 1966)

Fig. 2.3

From Figs. 2.3 and 2.4 we can see the fundamental difference between the behaviour of f-plane, and of β-plane situations. The variability of f provides the restoring force that

allows waves to exist far from the obstacle. In the f-plane case only one vorticity dipole is produced by the obstacle and, in this case, the cyclonic vortex sheds from the obstacle leaving the anticyclone standing over the mountain.

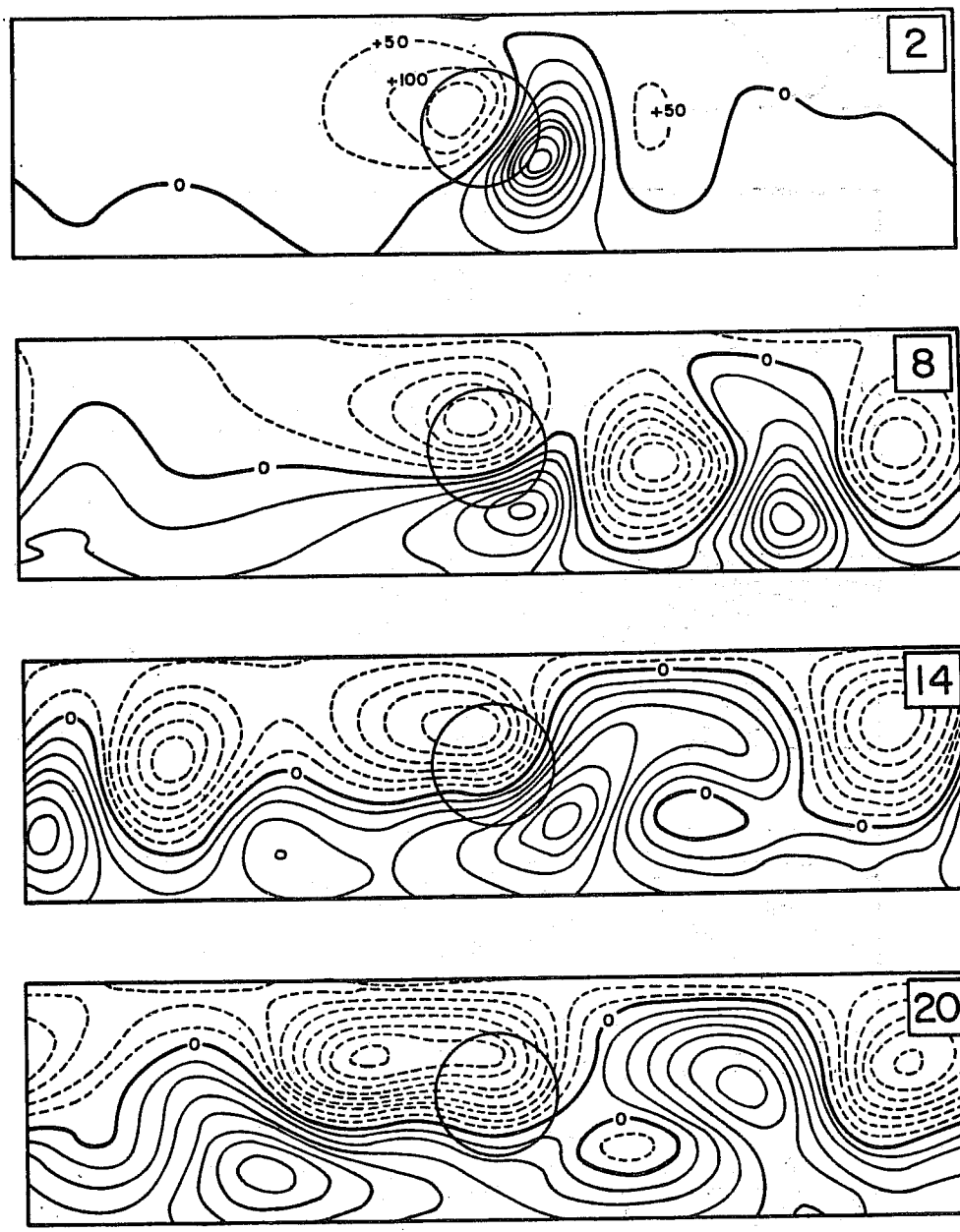

Variable f, U = 20 m/s

Evolution of height deviation field of Case B. Notice remarkable differences between Cases A and B. (After Kasahara, 1966)

Fig. 2.4

Easterly flow in a β-plane resembles more the solution for westerly flow in an f-plane (compare Figs. 2.3 and 2.5). This is due to the fact that the perturbations, induced by the obstacle decay exponentially in space for easterly flow, while they exhibit wavelike oscillations for westerly flow.

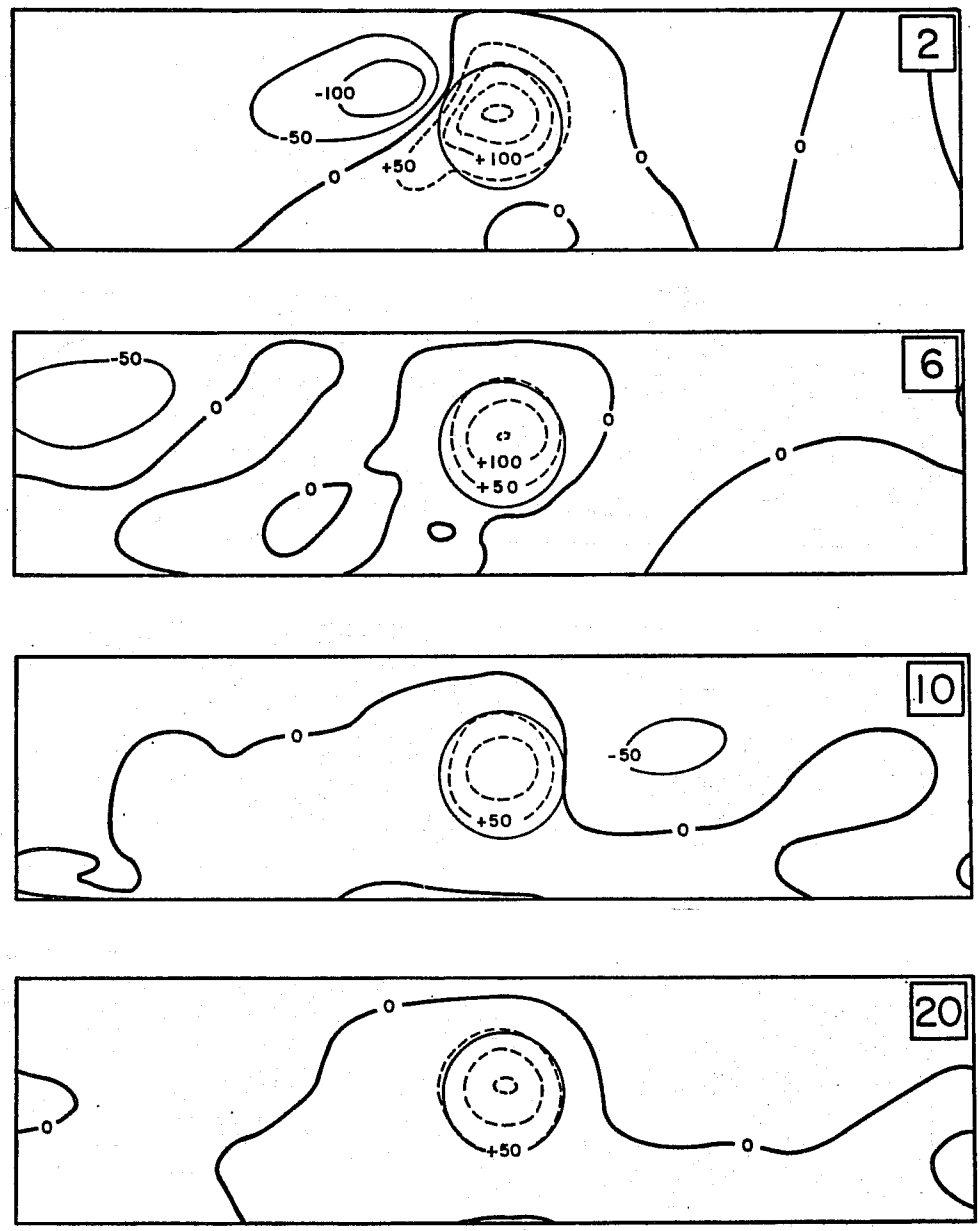

Variable f, U = - 20 m/s (easterly case)

Evolution of height deviation field of Case C. Observe remarkable differences between Cases B and C. (After Kasahara, 1966)

Fig. 2.5

The last consideration that we will make comparing Figs. 2.4, 2.6 and 2.7 is that, in accordance with theoretical considerations, the horizontal scale of variation of the mountain-induced perturbation (the wavelength, for the westerly-flow case) increases with $\bar{u}$.

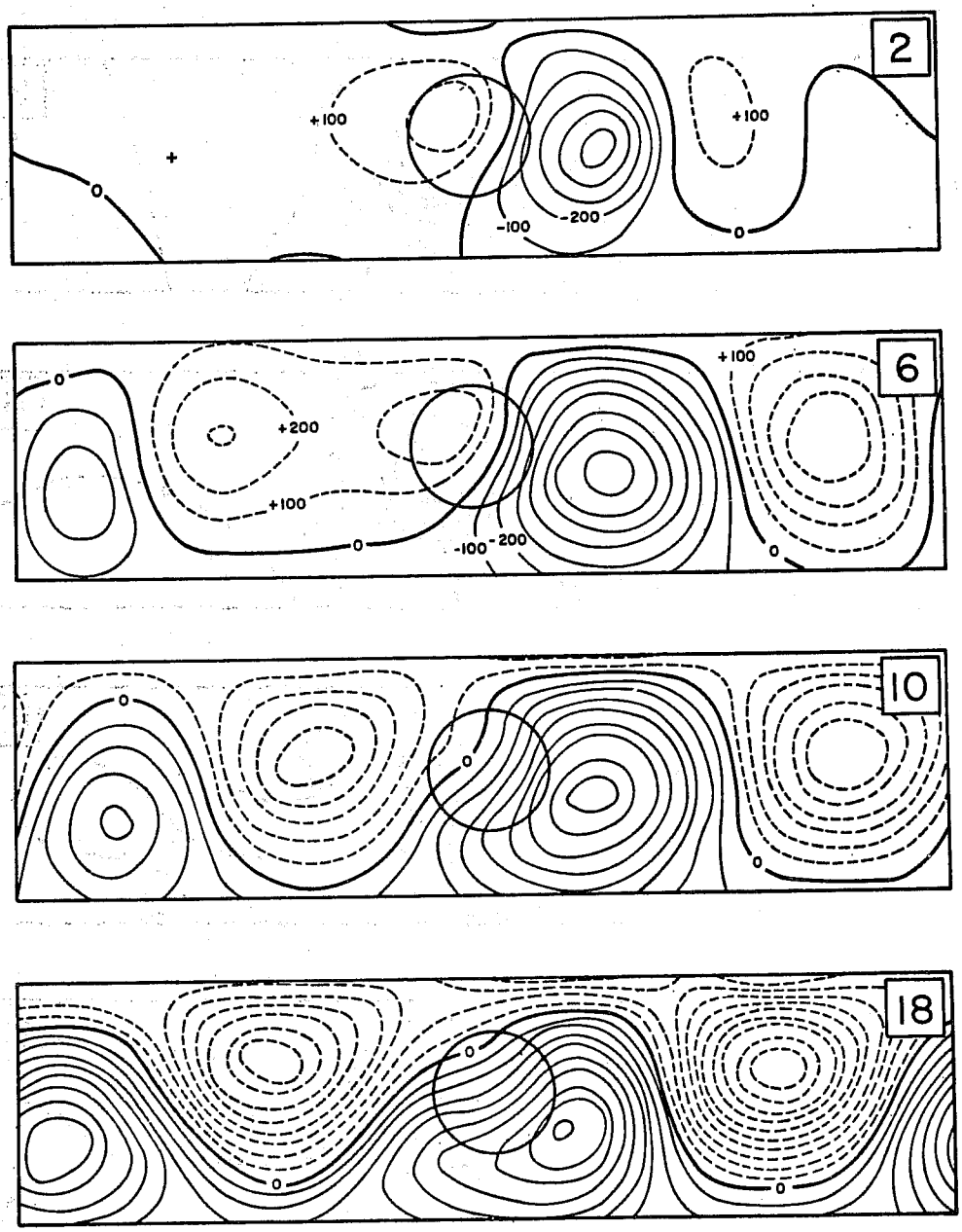

Variable f , U = 40 m/s

Evolution of height deviation field of Case D. Contours in this case are drawn for every 100-m interval. (After Kasahara, 1966)

Fig. 2.6

If we remember the Rossby-Haurwitz wave formula for the phase speed of the waves

$$c = \bar{u} - \frac{\beta + \lambda^2 \bar{u}}{k^2 + m^2 + \lambda^2} \qquad \lambda^2 = \frac{f_o^2}{gh_o} \qquad 2.3$$

k and m being the wavenumbers in x and y directions

$$k = \frac{\pi}{L_x} \quad ; \qquad m = \frac{\pi}{L_y} \quad .$$

Setting c = 0 (stationary waves), one obtains:

$$k^2 + m^2 = \frac{\beta}{\bar{u}} \qquad 2.4$$

that expresses the relationship between wavenumber and $\bar{u}$.

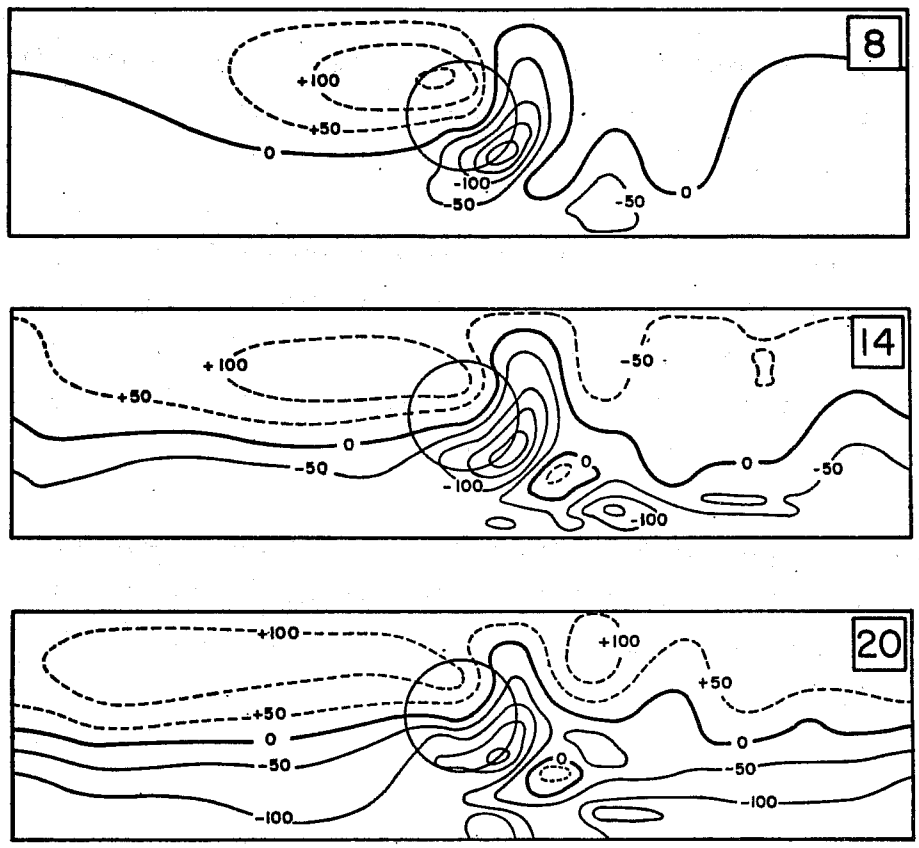

Evolution of height deviation field of Case E.
(After Kasahara, 1966)

Fig. 2.7

3. LINEAR MODELS OF LARGE-SCALE TOPOGRAPHIC FORCING

Several attempts of simulating the large-scale orographic and/or thermal forcing have been made by means of linearized model atmospheres, see e.g. Charney and Eliassen (1949), Bolin (1950), Smagorinsky (1953), Gilchrist (1954), Derome and Wiin-Nielsen (1971), Egger (1976), Grose and Hoskins (1979).

The linear approach allows to superimpose solutions and makes therefore meangingful the question as to whether the topographic forcing is more important than thermal forcing in determining the general behaviour of the westerlies, at least in terms of which of the two alone provides a better representation of the large-scale standing waves that are superimposed to the zonally averaged westerlies.

To show the extent to which this comparison is meaningful we will use the results obtained by Derome and Wiin-Nielsen (1971).

Fig. 3.1 shows the effects of topographic forcing (a), thermal forcing (b) and the two together (c) on the height of the 750 mb, 500 mb and 250 mb surfaces, compared with the observed distribution for January 1962, as averaged between 30^{o} and 60^{o} N.

The model is quasi-geostrophic, linear and steady-state and to the zonal current is superimposed a perturbation with a single meridional wavelength (mostly 60^{o} of latitude).

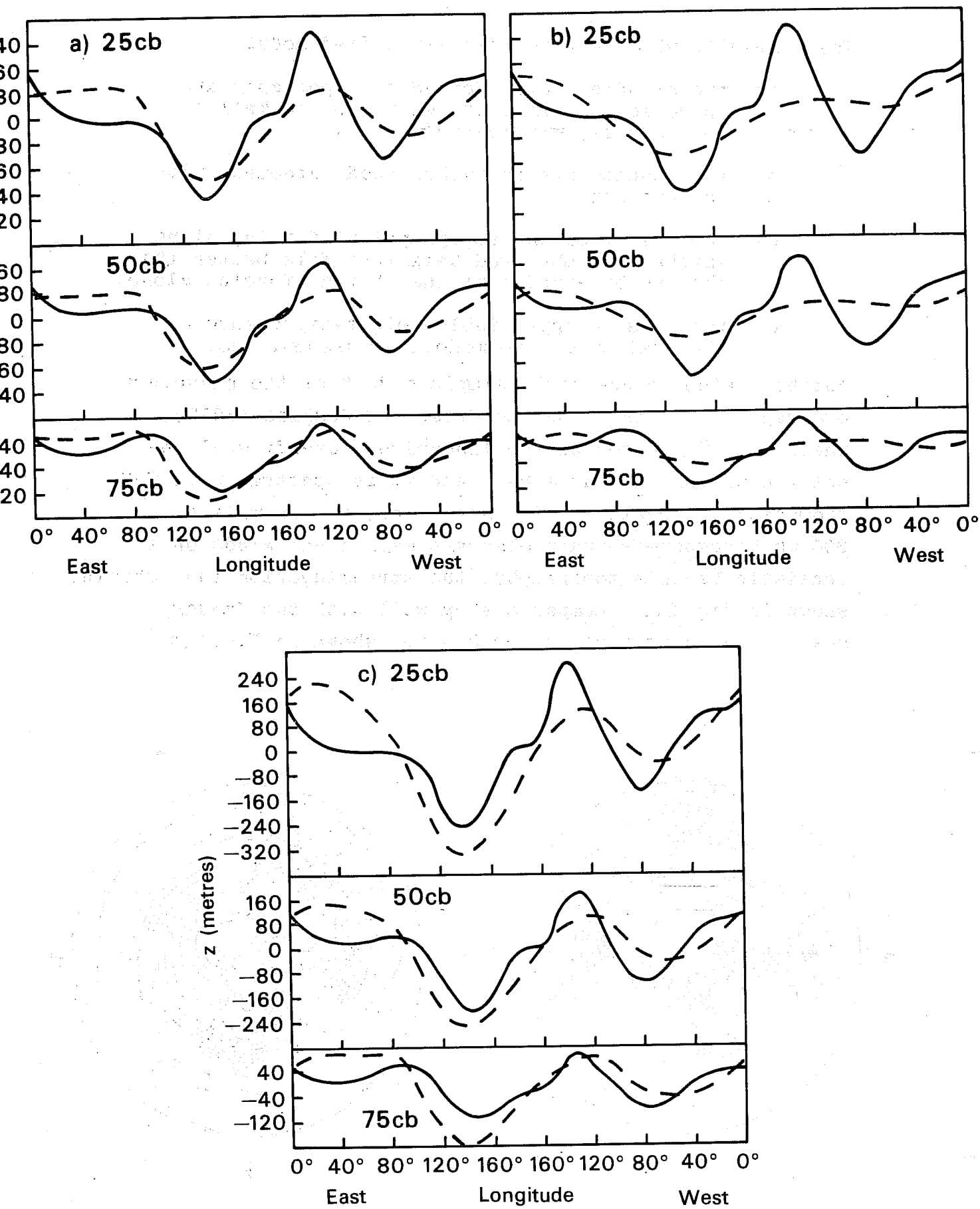

Figure 3.1 Perturbation heights of the 25, 50 and 75cb surfaces. Solid curves: observed distribution for January 1962, as averaged between 30° and 60°N. Dashed curves: a) Perturbation produced by the flow of zonal current over the distribution of standard pressure at the ground b) Perturbation produced by the diabatic heating c) Response of the model to the combined forcing of topography and diabatic heating. (After Derome and Wiin-Nielsen, 1971)

Their results show that in this simplified model:

a) the standing waves forced by topography are approximately in phase with the thermally forced ones, (in winter),

b) the results are in rather good agreement with observations,

c) the result of the topographical forcing alone matches the observed height profile better than the one obtained from the thermal forcing alone,

d) there is no appreciable height-dependence of the quality of the modelling assumptions.

Another rather successful "simple model" of the planetary orographic forcing is due to Grose and Hoskins (1979). Their model is based on the linearized, steady shallow-water equations on the sphere and it is spectral with T32 rhomboidal truncation. If they force, for example a 300 mb December-February observed mean zonal winds on a realistic Earth's topography, the streamfunction they obtain, shown in Fig. 3.3 , compares very well with the January mean height distribution for 300 mb, shown in Fig. 3.2.

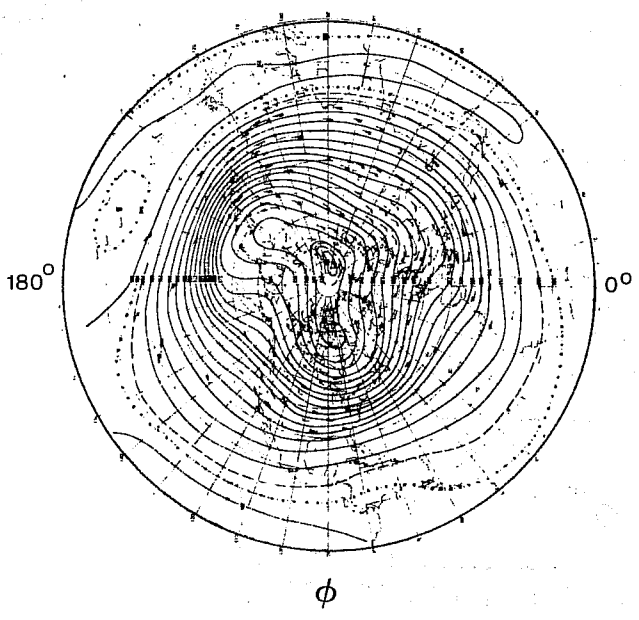

Fig.3.2 January 300 mb height (After Crutcher and Meserve, 1970)

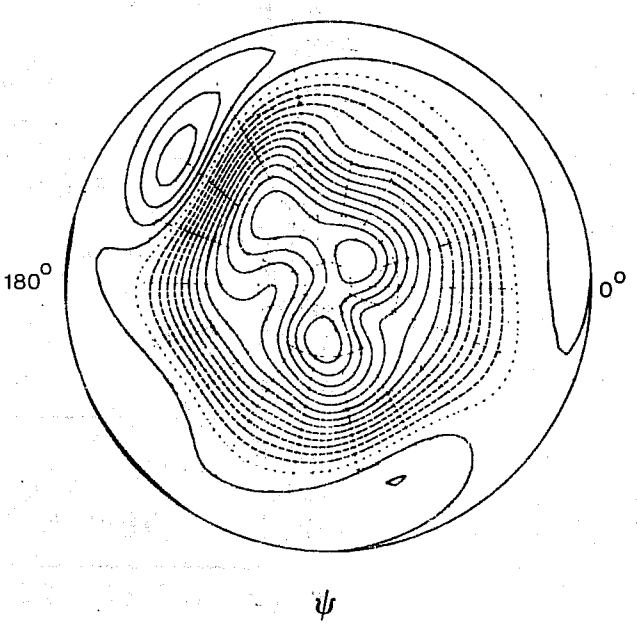

Fig.3.3 Streamfunction obtained forcing the 300 mb December-February observed mean zonal wind structure on the Earth's topography, linearised shallow water equations. (After Grose and Hoskins, 1979).

Simulations are less successful at other levels or for other months of the year.

It is likely that the good agreement obtained by this simple model is linked to the fact that, as mentioned above, for the shallow water equation set it is possible to derive a theorem of conservation of potential vorticity very similar to that valid for the adiabatic atmosphere; as we will see later, there are also reasons for believing that, while thermal forcing is particularly important for the low-level standing waves, the orographically-forced component may be the more important in the upper troposphere and stratosphere, and this fact could also be held partially responsible for the striking resemblance of Figs. 3.2 and 3.3.

We will now turn our attention to the problem of planetary mountain forcing in General Circulation Models.

When models become fully non-linear, as large GCM are, it becomes impossible to isolate all the different effects of a single model component (like orographic or thermal forcing), because non-linear interactions and feed back processes make this problem impossible even to pose.

The comparison between runs with and without a single "module" will however, still provide us with useful information about the cumulative effect of that particular feature on the model; how this is representative of the behaviour of the real atmosphere, will always be a matter of much speculation.

Such experiments are usually very expensive, both in terms of computer time and of manpower devoted to prepare the suitable diagnostic tools and to interpret the results, and this is probably the reason why not many experiments of this kind have been attempted.

We will mention here, without any pretence of completeness, the experiments carried out using the NCAR GCM (Kasahara and Washington, 1971, Kasahara, Sasamori and Washington, 1973), the GFDL (Manabe and Terpstra, 1974) and the UK Meteorological Office 6-level GCM (Rowntree, 1975, Hills, 1979). We will try to review results that appear to be of significance, more than drawing conclusions, not so easy to extract from the so far composite picture.

4. THE NCAR EXPERIMENTS

This experiment was performed in two steps; first of all the NCAR 6-level GCM was run up to 80 days with (M-experiment) and without orography (NM-experiment) to simulate January climate starting from an isothermal atmosphere at rest. Than, to evaluate the role of the topography on the stratospheric general circulation, and to improve the troposphere simulation bringing the artificial top boundary condition further up, the experiment was repeated with a 12-level model, for which the lowermost six levels were coincident with the previous 6 levels. Both models were global, had a 5^{o} lat-lon grid and used z as vertical coordinate, and had, therefore, mountains inserted through somewhat artificial boundary conditions. The authors state that the comparison between the two experiments shows that "the addition of the stratosphere over the troposphere improves the description of the upper troposphere circulation" as was expected.

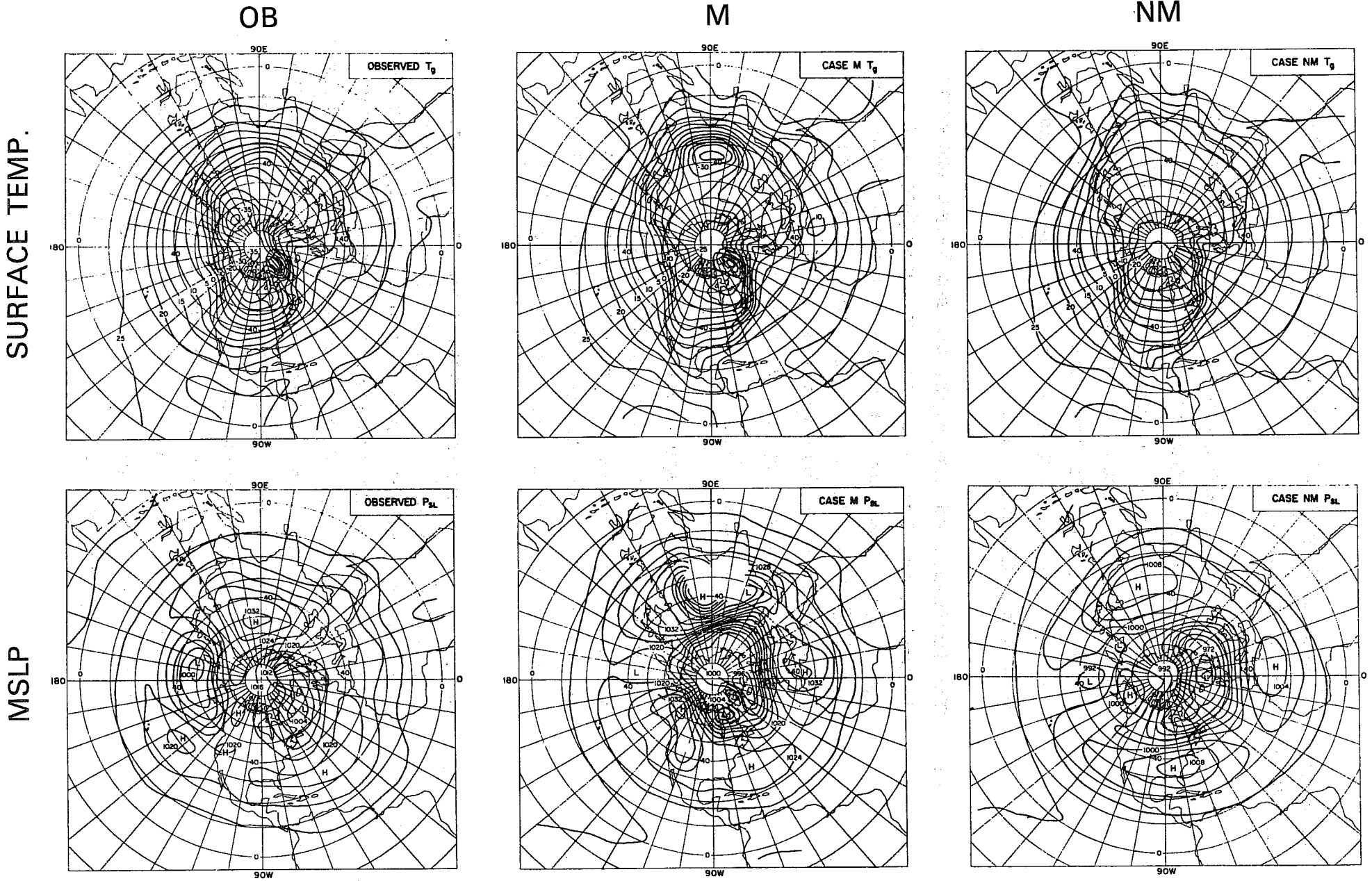

Fig. 4.1 Geographical distributions of sea-level pressure (contour interval of 4 mb) and surface temperature (contour interval, 5°C) for a 30-day mean computed for Case NM, a 30-day mean computed for Case M, and the observed distribution for January for the northern hemisphere. (After Kasahara et al, 1971 and 1973).

The main conclusions they reach comparing the M-runs with the NM-runs are the following:

a) Obviously, the inclusion of orography helps to bring the calculation of the ground surface temperature closer to reality, particularly over the mountainous regions such as Greenland and Antarctica. On the other hand, we note that the Himalayan Plateau is much colder than observed. See Fig. 4.1.

b) The influence of orography on sea level pressure distribution (Fig. 4.1) is not inserting any immediately obvious improvement and is probably influenced by its being a somewhat artificial production (reduction methods). Upper-level wind fields are very little influenced by the insertion of mountains.

c) The earth's orography seems to have a large influence on the pressure pattern in the mid-stratosphere, developing the Aleutian high (see Fig. 4.3), while its effects on the lower stratosphere are not so visible (Fig. 4.2).

d) As far as tropospheric zonal mean states are concerned, the dynamic effect of the earth's orography does not appear to be a major influencing factor in determining the zonal statistics for January. In the N.H. stratosphere significant (positive) effects of the insertion of the earth's orography are seen in the thermal structure of the polar lower stratosphere. The reason for the colder temperature over the North Pole in the stratosphere in the N.M. case seems to be due to smaller horizontal heat transport by planetary-scale eddies.

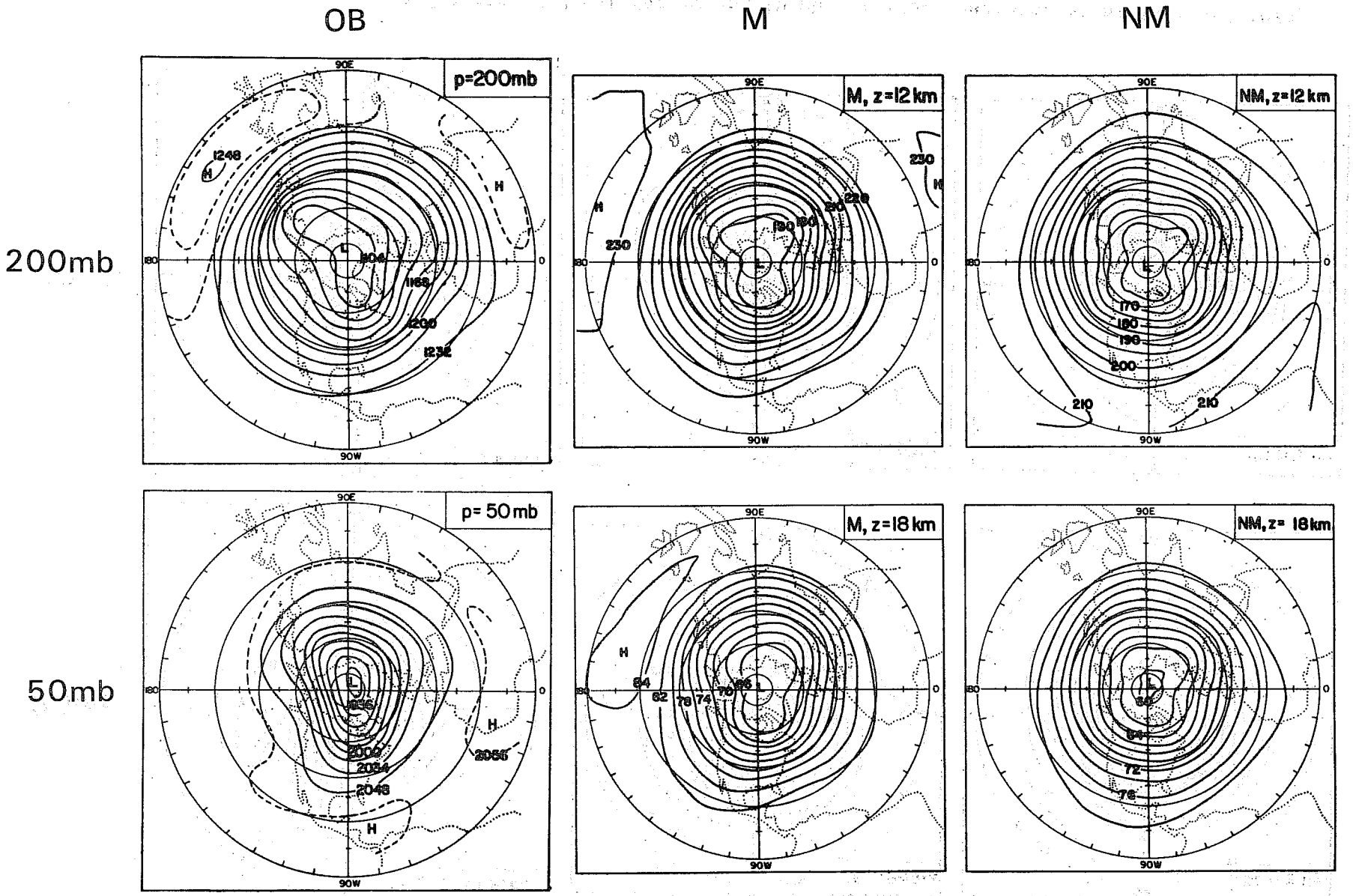

Fig.4.2 Left: mean January Northern Hemisphere (N.H.) geopotential distributions (dkm) at 200 and 50 mb. Centre: computed 30-day mean pressure distributions (mb) at 12,18, 24 and 30 km in the N.H. for Case M. Right: same as for centre but for Case N.M. (After Kasahara, et al 1971 and 1973)

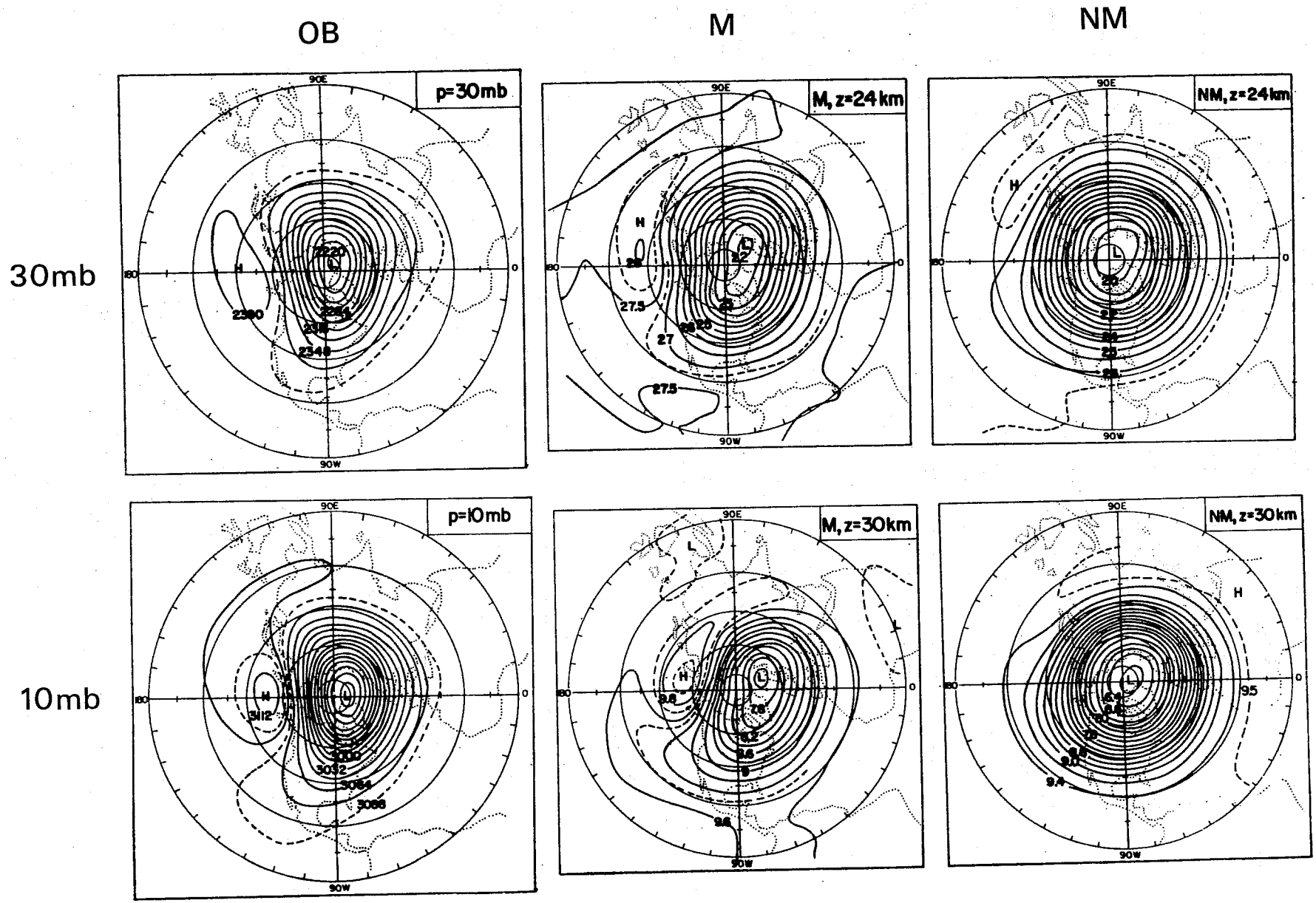

Fig. 4.3 Same as for Fig. 4.2 but for 30 and 10 mb. (After Kasahara, et al 1971 and 1973)

See Fig. 4.4. To investigate the effect of orography on the eddy transports of momentum and sensible heat in detail, they present in Figs. 4.5 a) and b) the latitudinal distributions of $\overline{u'v'}$ and $\overline{v'T'}$, respectively, at different height levels for Cases M and NM. The scale of the ordinates changes at different vertical levels. The orography does not significantly change the northward eddy flux of momentum except for the upper three levels in the N.H. and the lower four levels in the S.H. On the other hand, the orography significantly increases the northward transport of sensible heat $\overline{v'T'}$ from the N.H. stratosphere down to the middle-latitude region of the upper troposphere.

e) Concerning the question of the relative importance between the thermal effect of continentality and the dynamic effect of orography in determining the large scale features of climate, these experiments indicate that the thermal effect is the dominating factor for simulation of the tropospheric January climate. However, the dynamic effect of the earth's orography is a dominant factor in reproducing the Aleutian high in the the stratosphere which characterizes the circulation in the N.H. stratosphere during wintertime.

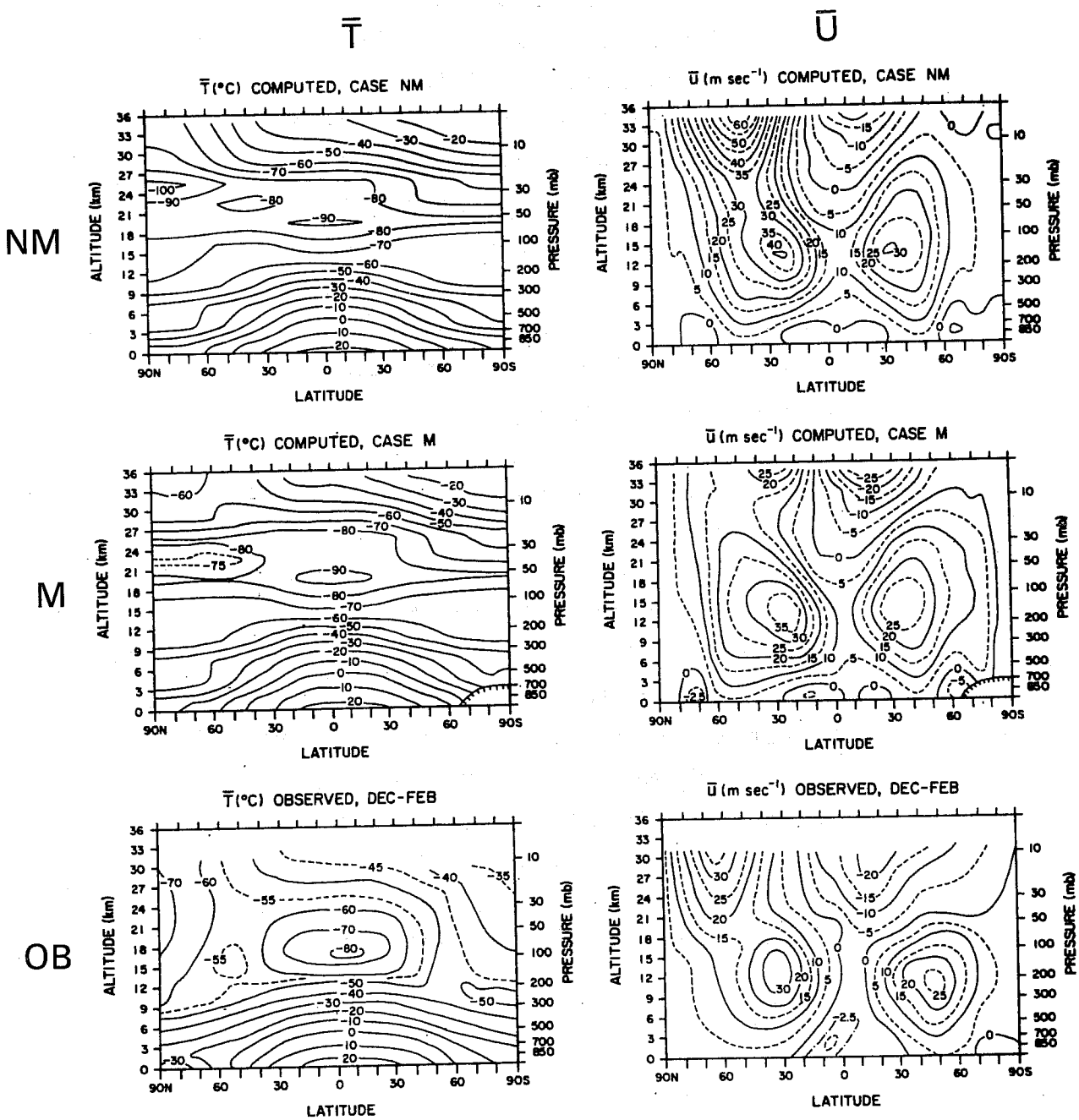

Fig. 4.4 Left: from the top down, zonally averaged mean temperature cross sections of Case NM, Case M, and observed long-term mean. Right: zonally averaged mean west-to-east velocity component cross sections of Case NM, Case M, and observed long-term mean.

(After Kasahara et al 1971 and 1974)

$\overline{U'V'}$

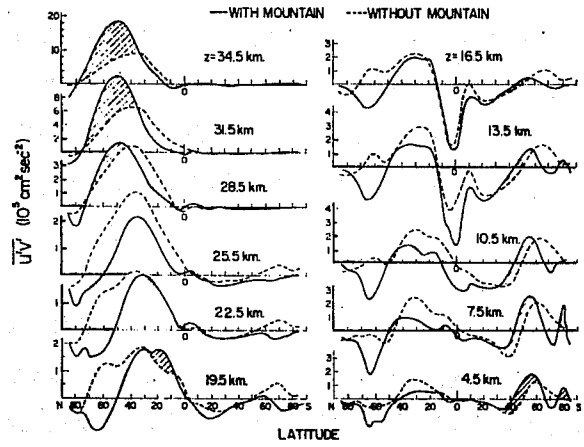

a)

Latitudinal distributions of $\overline{u'v'}$ at different levels for Case M and Case NM. The increase of northward transport of westerly momentum due to mountains is indicated by crosshatching.

$\overline{V'T'}$

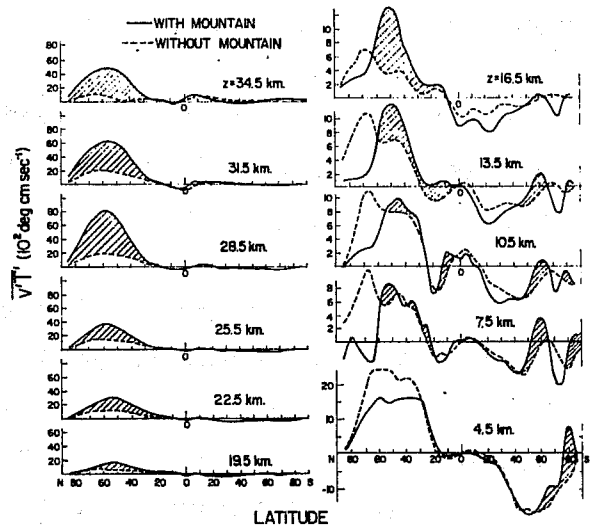

b)

Same as above but for $\overline{v'T'}$.

Fig.4.5 (After Kasahara et al 1971 an 1973)

5. THE GFDL EXPERIMENTS

This experiment, reported by Manabe and Terpstra (1974), provides the, up to now, most complete and extensive comparison between a "mountain" (M) and a "no-mountain" (NM) GCM run, with the aim of identifying the effects of mountains upon the general circulation of the atmosphere and discussing the role of mountains in maintaining the stationary and transient disturbances in the winter atmosphere.

The model is a 9-level, primitive equation, global σ-model on a Kurihara-type grid with horizontal grid size of approximately 250 km. The M-run was initiated from a zonal mean state (obtained from a previous hemispheric run) and integrated with a coarse ($\frac{1}{2}$) resolution for 302 days. The integration was then continued for 70 days at maximum resolution. The NM-run was started from the 60th day of the high resolution M-run and integrated for 62 days. Averages were taken on the last 40 days periods of the two runs.

The conclusions that the authors derived after the comparison between the M-model atmosphere and the NM-model atmosphere are the following.

1. In general, the distribution of the stationary flow field in the M-model atmosphere is more realistic than that in the NM-model atmosphere. The effects of mountains are indispensable for the successful simulation of the stationary flow field, particularly in the upper troposphere and stratosphere. On the other hand the thermal effects seem to be important in the lower troposphere.

2. The distribution of the mean geopotential height of the isobaric surfaces in the upper troposphere of the M-model shows that a stationary trough is located in the lee of major mountain ranges such as the Tibetan Plateau and the Rocky Mountains. The trough tilts from southwest to northeast indicating the northward transport of angular momentum. The area of maximum westerlies appears to the east of the trough. See Figs. 5.2 a) and 5.3.

3. An intense stationary cyclone forms over the Aleutian Archipelago in the lower troposphere of both the M and NM models. This result suggests that the mountains are not necessary for the formation of the Aleutian low. (Fig. 5.1).

4. The Tibetan Plateau is responsible for the intensification and the northward shift of the lower tropospheric anticyclone over the Eurasian continent. In other words, it plays a very important role for the maintenance of the Siberian high. (Fig. 5.1).

5. The M-model simulates successfully some of the qualitative features of the stationary flow in the stratosphere such as the Aleutian anticyclone and the intense trough over the North American continent. However, the intensity of the zonal wind in the model stratosphere is much stronger than the observed wind. The flow field in the NM-stratosphere appears to be more zonal and is much less realistic though it fails to reach a quasi-steady state toward the end of the time integration. (Figs. 5.2 and 5.4).

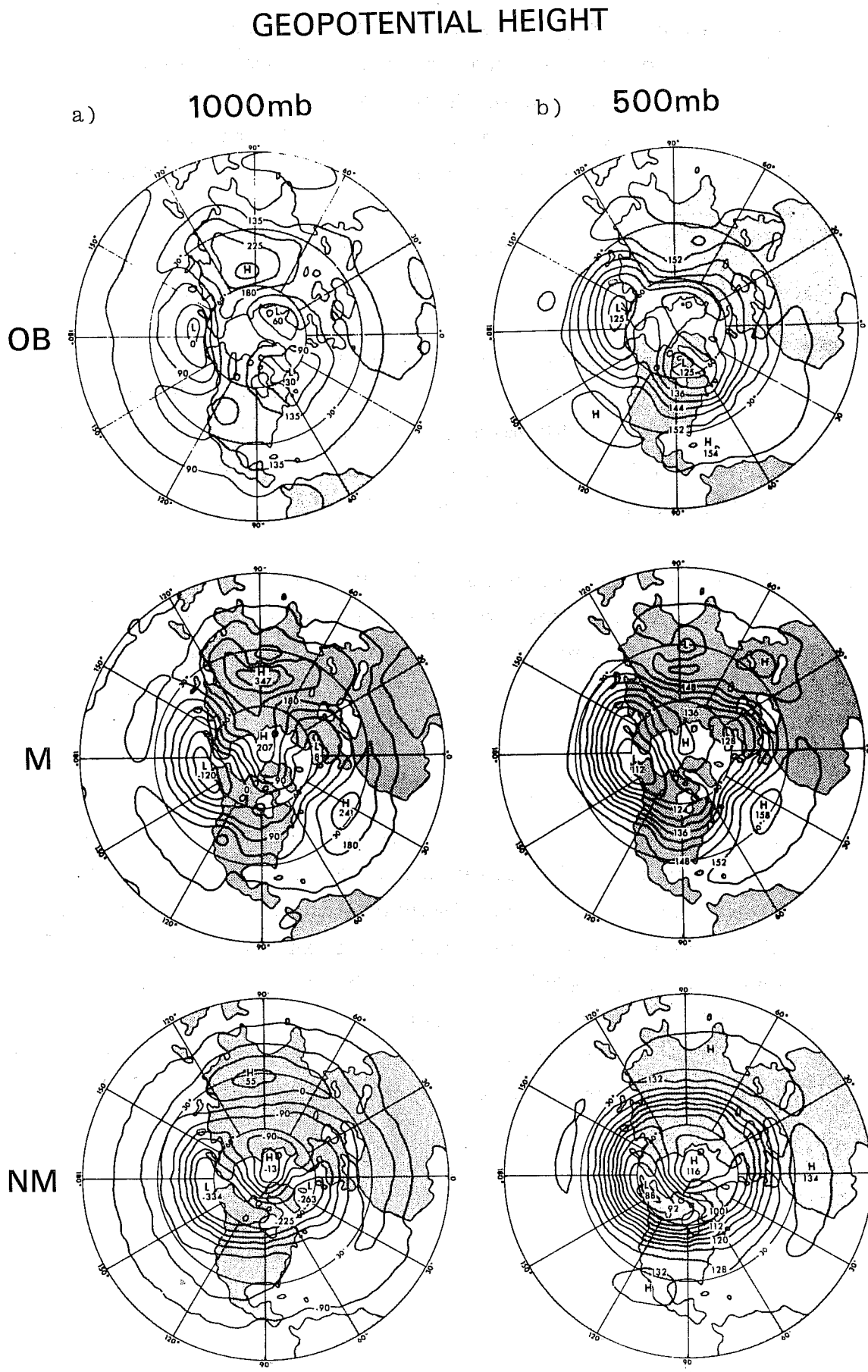

Fig.5.1 Time-mean geopotential height maps of the Northern Hemisphere at 1000 mb (left) and 500 mb (right). Units for 1000 mb case, geopotential meters; and for 500 mb case, geopotential decameters. Top: observed (Oort and Rasmusson (private communication); average over five Januaries, 1959 - 63)); middle: the M model; bottom: the NM model. (After Manabe and Terpstra, 1974)

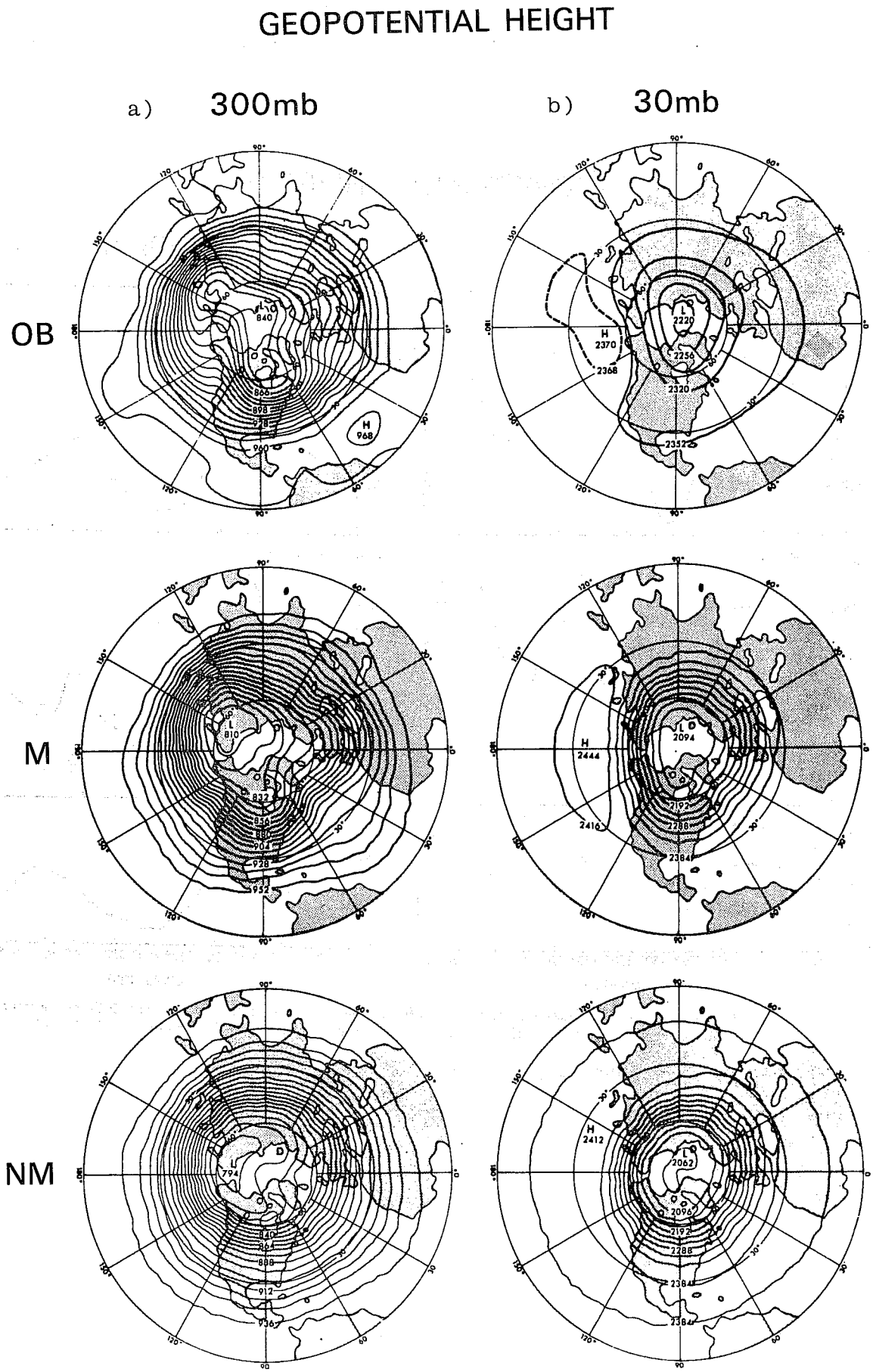

Fig.5.2 As in Fig. 5.1 except for 300 mb (left) and 30 mb (right): units, geopotential decameters. (After Manabe and Terpstra, 1974).

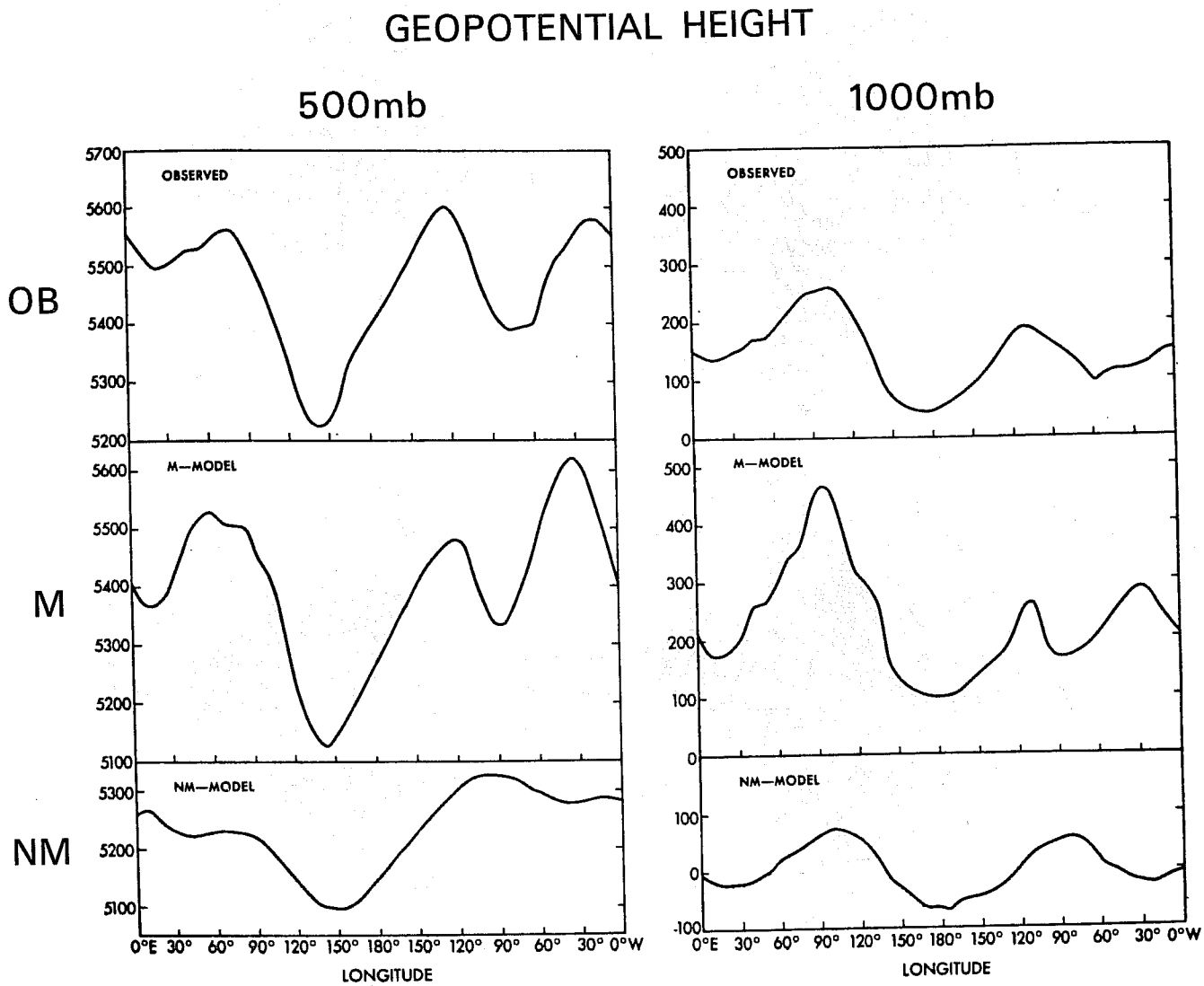

Fig. 5.3 Longitudinal variation of the time-mean geopotential height (geopotential meters) of 500- and 1000-mb levels at 45N: top, observed (Oort and Rasmusson, private communication); middle, the M-model; bottom, the NM-model.

(After Manabe and Terpstra, 1974)

ZONAL WIND $\bar{U}$

OB

M

NM

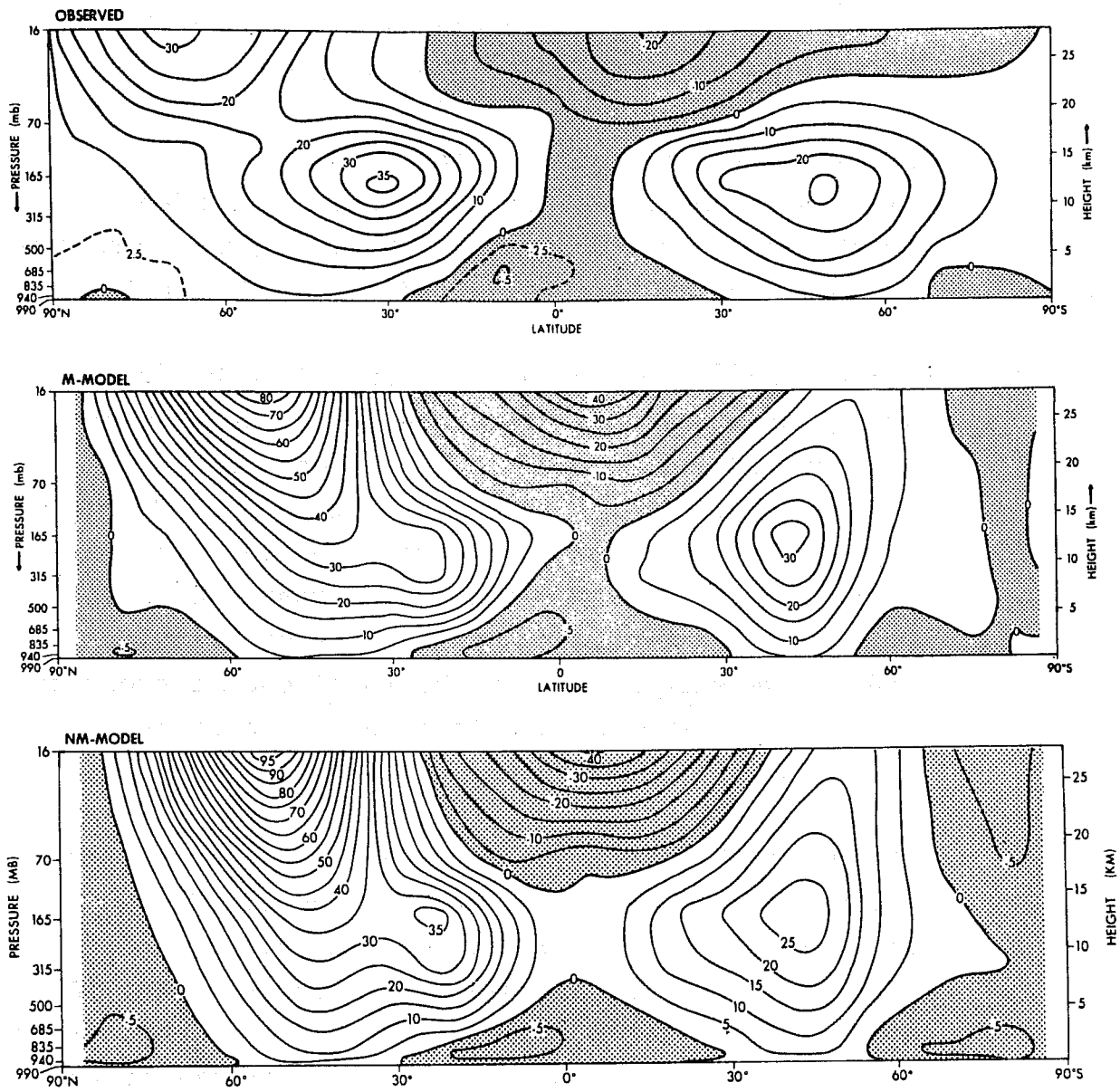

Fig. 5.4 The latitude-height distribution of the time mean zonal wind (m sec^{-1}): top, observed (Newell *et al.*, 1971); middle, the M-model; bottom, the NM-model.

(After Manabe and Terpstra, 1974)

6. The kinetic energy of stationary disturbances increases appreciably whereas that of transient eddies decreases as a result of incorporating the effects of mountains into the model. Because of these two compensating tendencies, the total eddy kinetic energy in the model troposphere is affected little by mountains. (See Figs. 5.5 and 5.6).

7. A similar tendency of compensation between the stationary and transient components is evident in the northward transport of heat, angular momentum and moisture by large-scale eddies. (Fig. 5.7).

8. The conversion of potential energy into kinetic energy of stationary disturbances in the Northern Hemisphere of the model increases markedly due to the incorporation of mountain effects. This is the major reason for the increase of the kinetic energy of stationary disturbances mentioned above. Mountains, however, reduce the rate of transient eddy conversion such that the total eddy conversion in the model troposphere is hardly altered due to the effects of mountains. (Fig. 5.8).

9. The wavenumber analysis of total eddy conversion indicates that mountains are responsible for appreciably increasing the longitudinal scale of eddy conversion in the model atmosphere. (Fig. 5.9 a). This increase chiefly results from the large increase of the stationary component of eddy conversion which takes place at very low wavenumbers. It should be pointed out that the characteristic scale of the transient component of eddy conversion also increases somewhat as a result of incorporating the effects of mountains.

In response to the increase of the characteristic scale of eddy conversion mentioned above, the longitudinal scale of the disturbance also increases significantly. Again, this increase mainly results from a marked increase of the kinetic energy of stationary eddies at very low wavenumbers (Fig. 5.9 b).

10. The energy exchange between the stratosphere and the troposphere through the stationary component of eddy pressure interaction is enhanced very much in the Norther Hemisphere upward wave propagation of the model by the effects of mountains. (Fig. 5.10). This is a major reason why the eddy kinetic energy of the stationary disturbances in the M-model stratosphere is much larger than that in the NM-model stratosphere. A secondary reason is the increase of stationary eddy conversion in high latitudes of the Northern Hemisphere of the model caused by the incorporation of mountain effects.

11. A major mountain range such as the Tibetan Plateau or the Rocky Mountains tends to increase the probability of cyclogenesis in the lee of the mountain range. (Fig. 5.11 and 5.12).

12. The distribution of the time-mean rate of precipitation in the M-model atmosphere is much less zonal and more realistic than that in the NM-model atmosphere. (Fig. 5.13).

KINETIC ENERGY

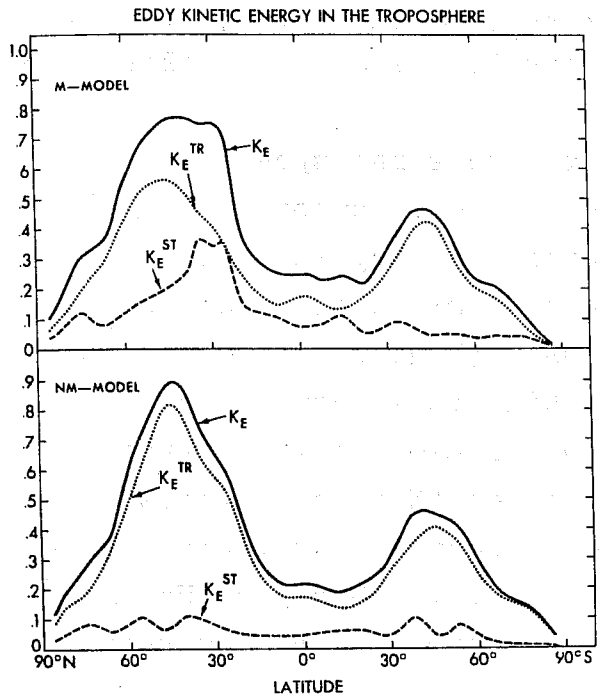

The latitudinal distribution of K_E (solid line), K_E^{ST} (dashed line) and K_E^{TR} (dotted line) integrated over the model troposphere in units of 100 J cm^{-2}. The troposphere is defined as the part of the model atmosphere below 240 mb. Top, the M-model; bottom, the NM-model.

(a)

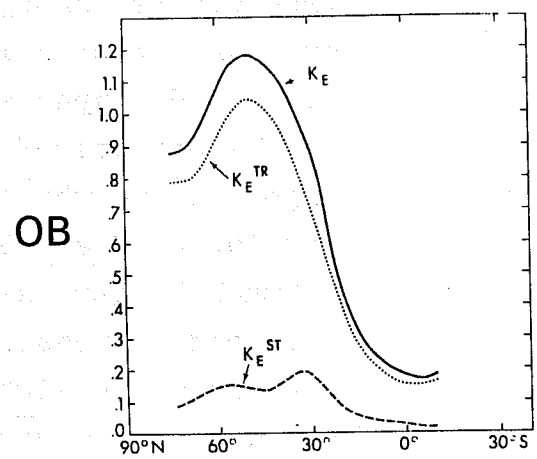

The observed latitudinal distribution of K_E, K_E^{ST} and K_E^{TR} integrated over the troposphere in units of 100 J cm^{-2}. The troposphere is defined as the part of the atmosphere below the 250-mb level. (After Oort and Rasmusson, 1971.)

(b)

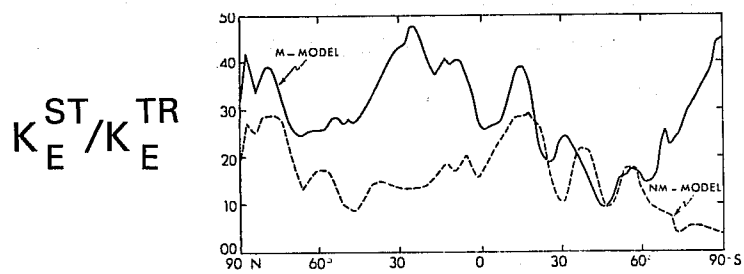

The latitudinal distribution of the ratio of K_E^{ST} to K_E^{TR}: M-model, solid line; NM-model, dashed line. (Here, K_E^{ST} and K_E^{TR} represent the mass integrals over the model tropospheres).

(c)

Fig.5.5 (After Manabe and Terpstra, 1974)

EDDY KINETIC ENERGY

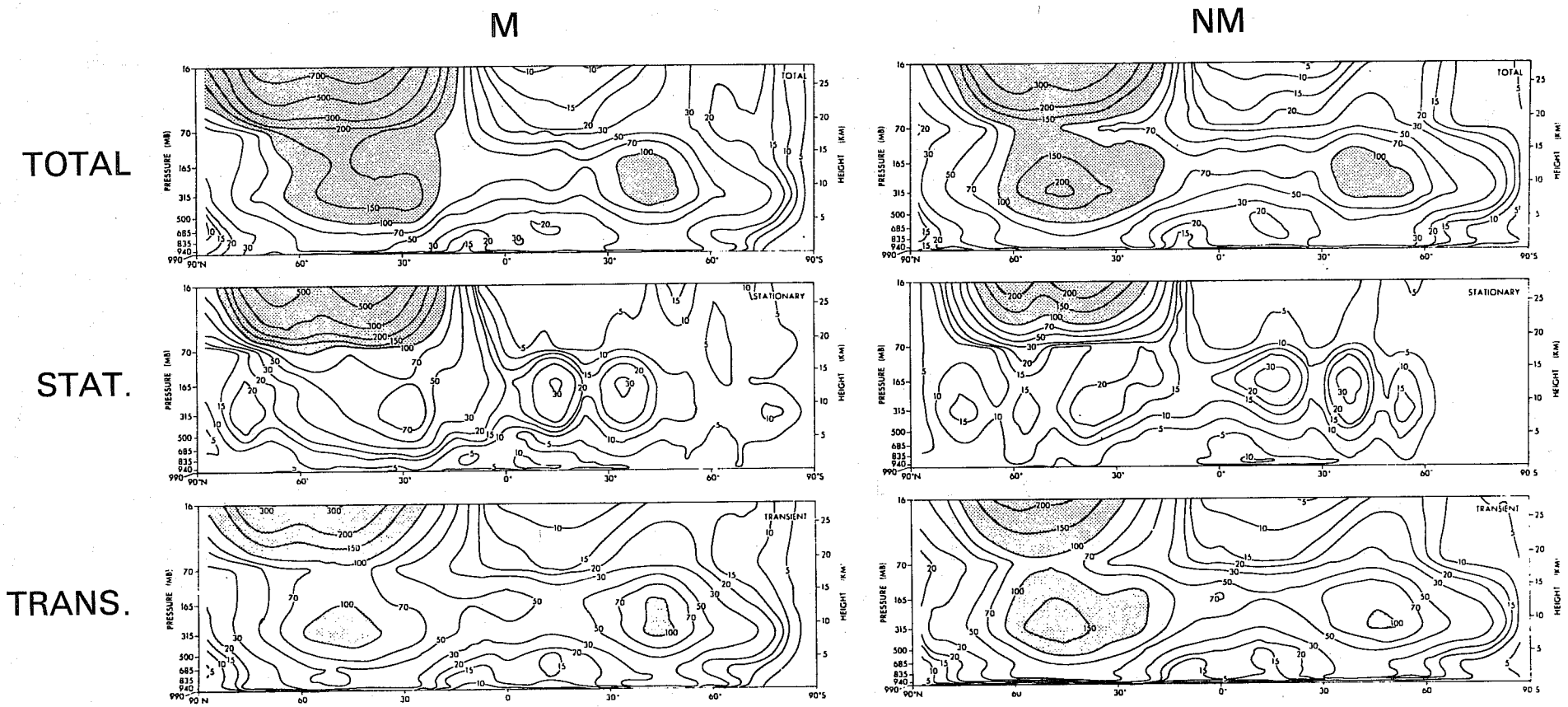

Fig.5.6 The latitude-height distribution of K_E, K_E^{ST} and K_E^{TR} (top, middle, bottom) for the M-model (left) and the NM-model (right): units, 10^{-3} J cm^{-2} mb^{-1}.

(After Manabe and Terpstra, 1974)

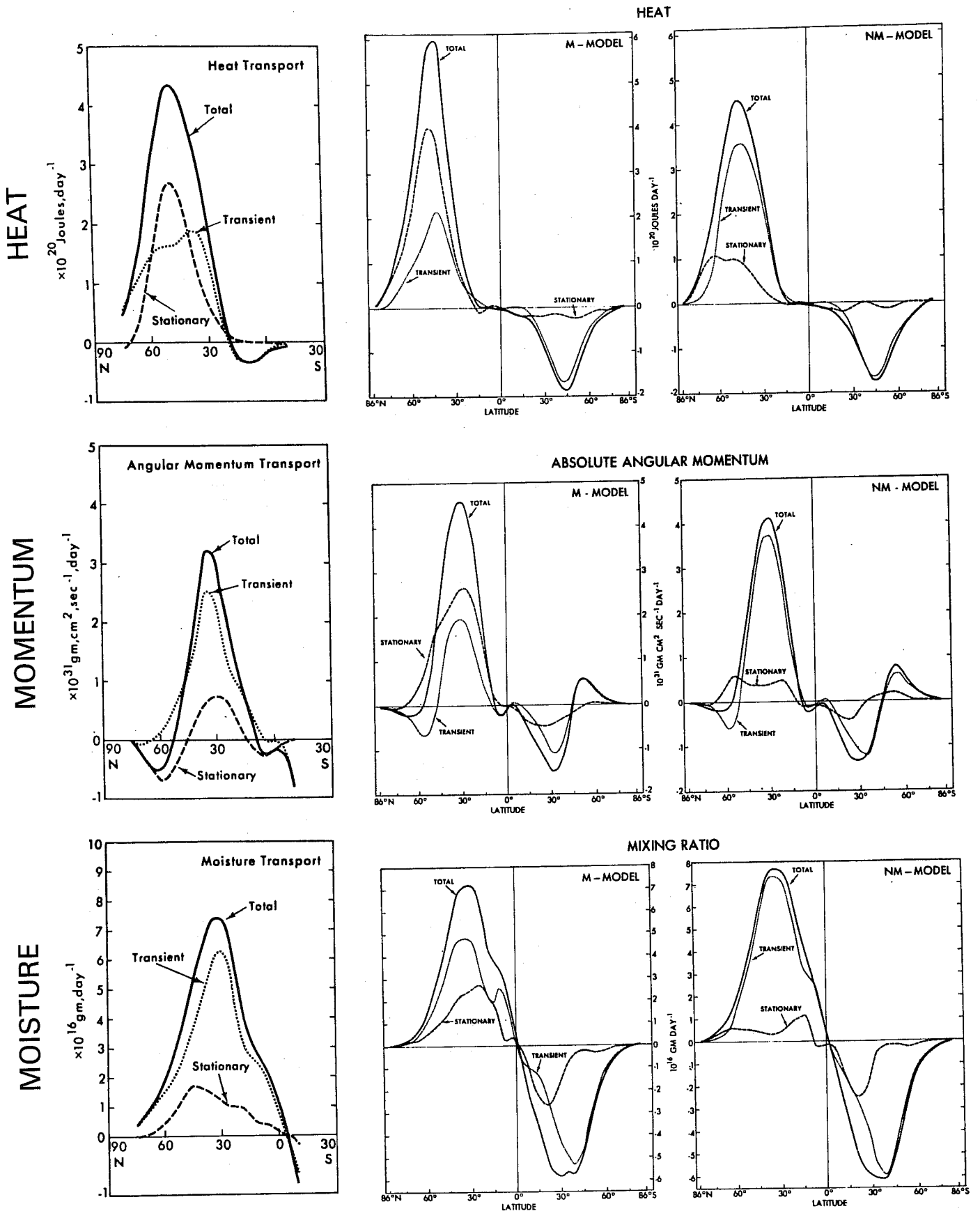

Fig. 5.7 Northward eddy transport (vertical integral) of heat (top) in units of 10^{20} J day^{-1}, angular momentum (middle) in units of 10^{31} gm cm^{-2}sec^{-1}, and moisture (bottom) in units of 10^{16} gm day^{-1}. Centre, the M-model; right, the NM-model; left, observed average over five Januaries

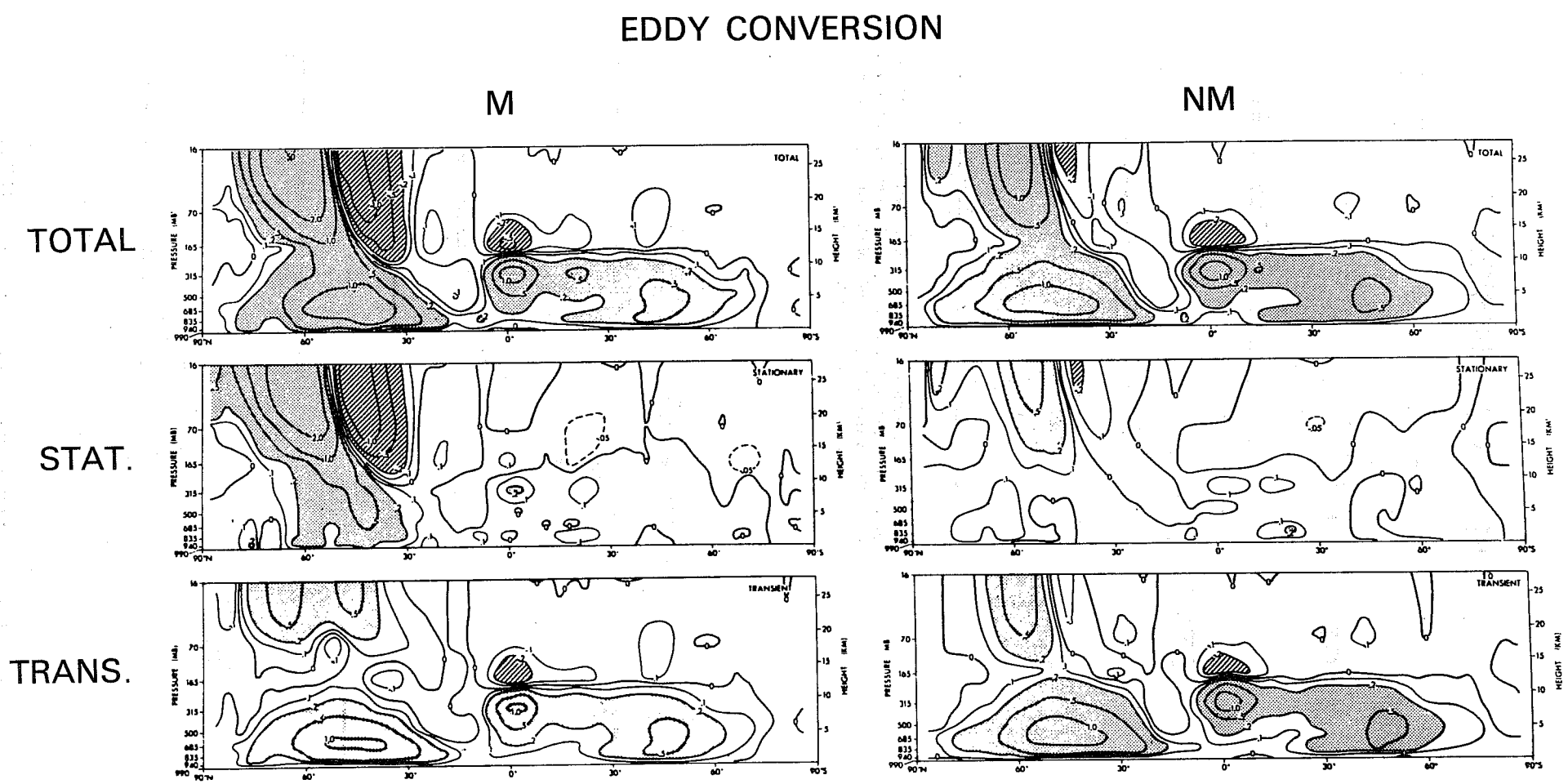

Fig.5.8 Latitude-height distribution of eddy conversion: left, the M-model; right, the NM-model. Top, total; middle, stationary; bottom, transient. Units: 10^{-1} J cm^{-2} mb^{-1} day^{-1}. (After Manabe and Terpstra, 1974)

a) EDDY CONVERSION

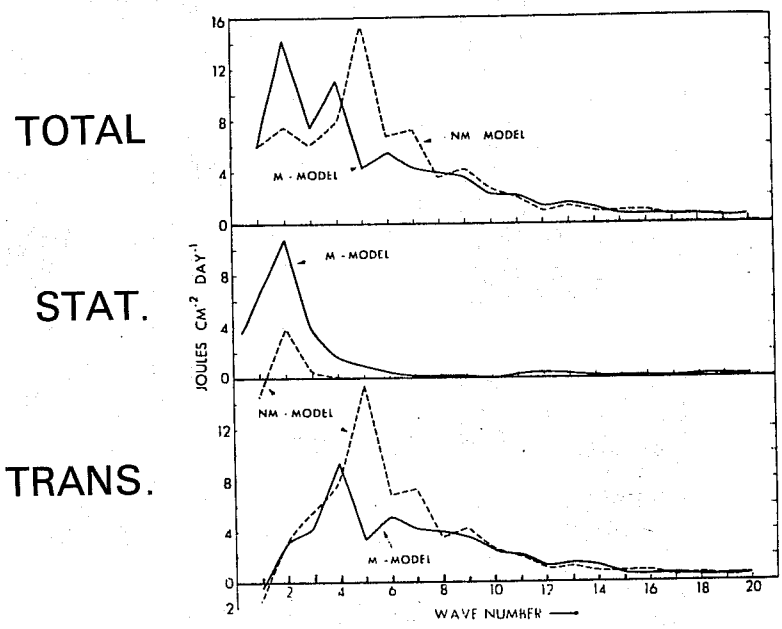

Spectrum of the vertical mass integral of eddy conversion for the latitude belt between 40 and 50N : solid line, M-model; dashed line, NM-model. Top, total; middle, stationary; bottom, transient. The vertical integral includes both the stratosphere and the troposphere.

b) EDDY KINETIC ENERGY

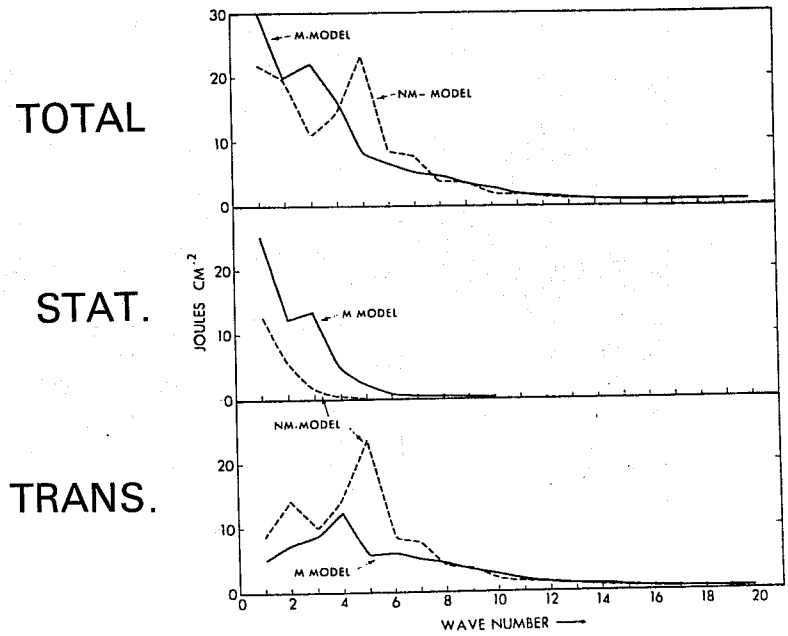

As above except for eddy kinetic energy.

Fig. 5.9 (After Manabe and Terpstra, 1974)

EDDY PRESSURE INTERACTION

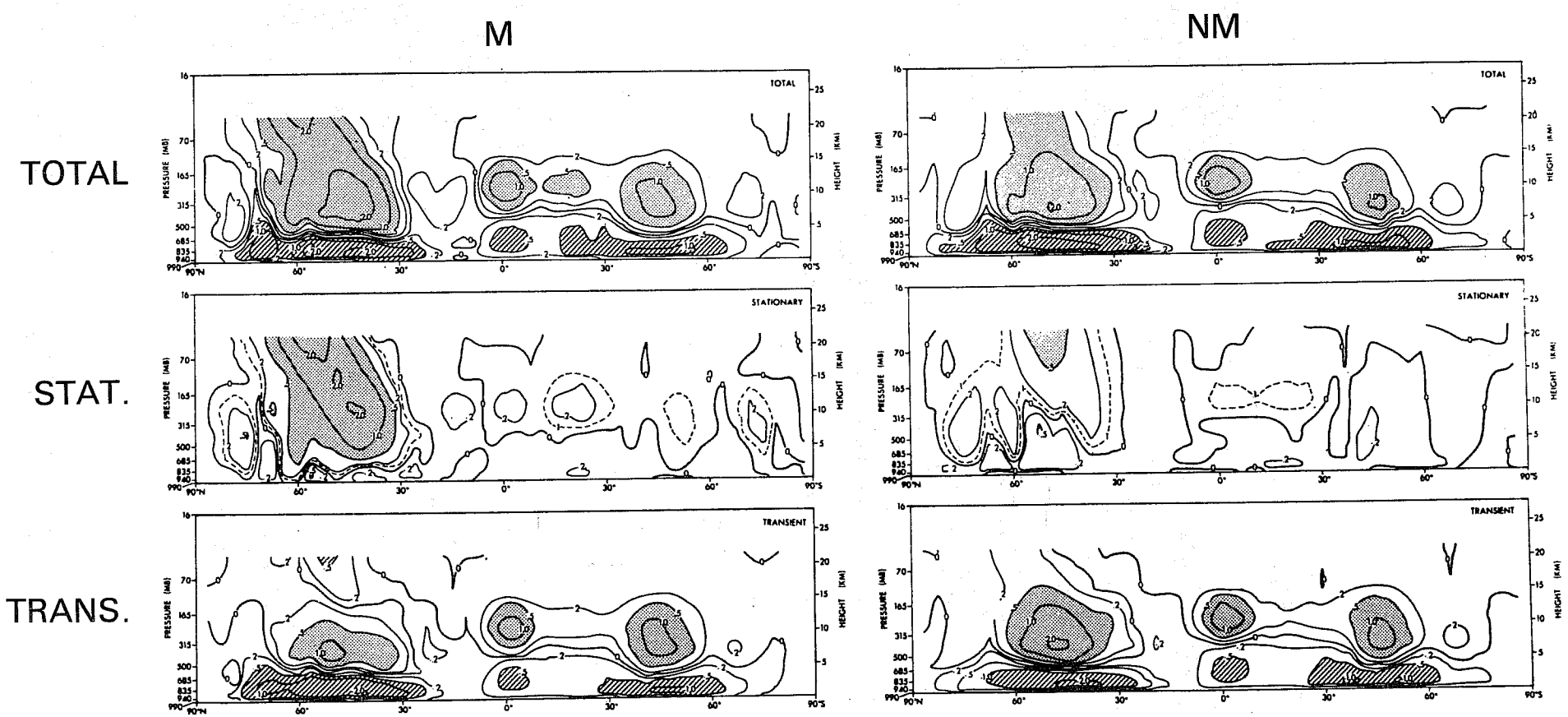

Fig.5.10 Latitude-height distribution of the vertical component of eddy pressure interaction: left side, M-model; right side, NM-model. Top, total; middle, stationary; bottom transient. Units, J cm^{-2} day^{-1}.

(After Manabe and Terpstra, 1974)

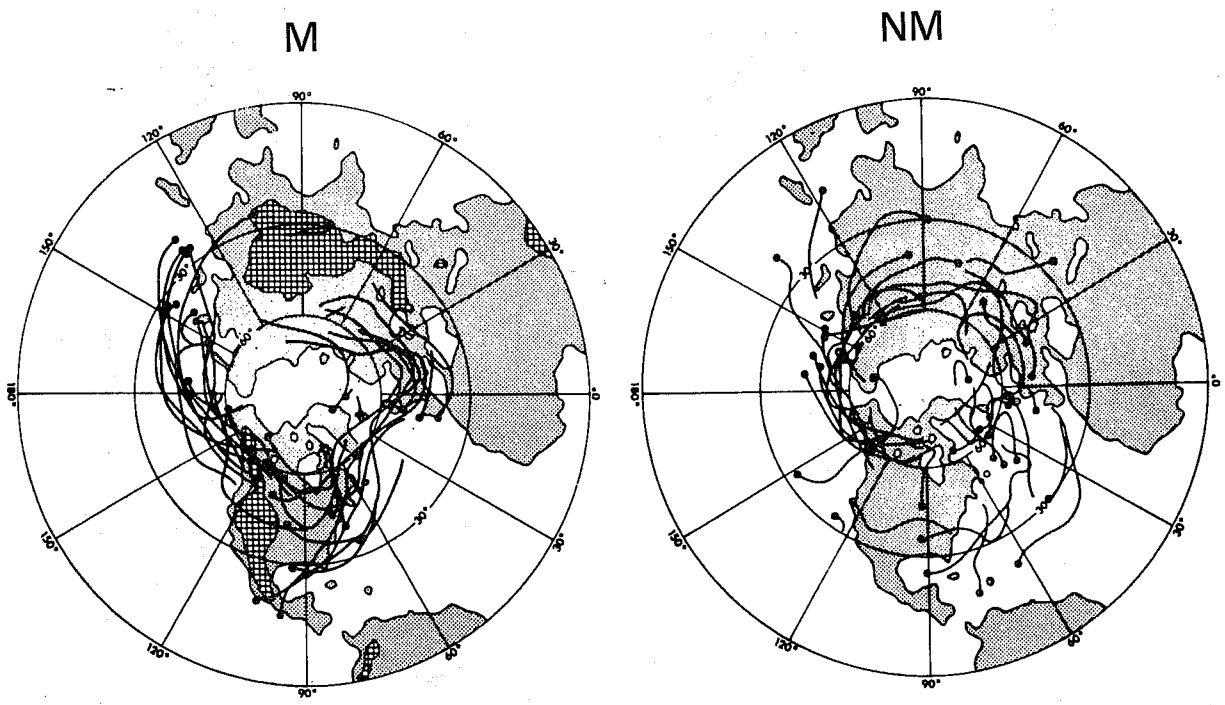

Computed streaklines of cyclones. Black dots indicate the approximate locations of cyclogenesis. The analysis period is 45 days for both models. Right side, the NM-model; left side, the M-model.

(After Manabe and Terpstra, 1974)

Fig. 5.11

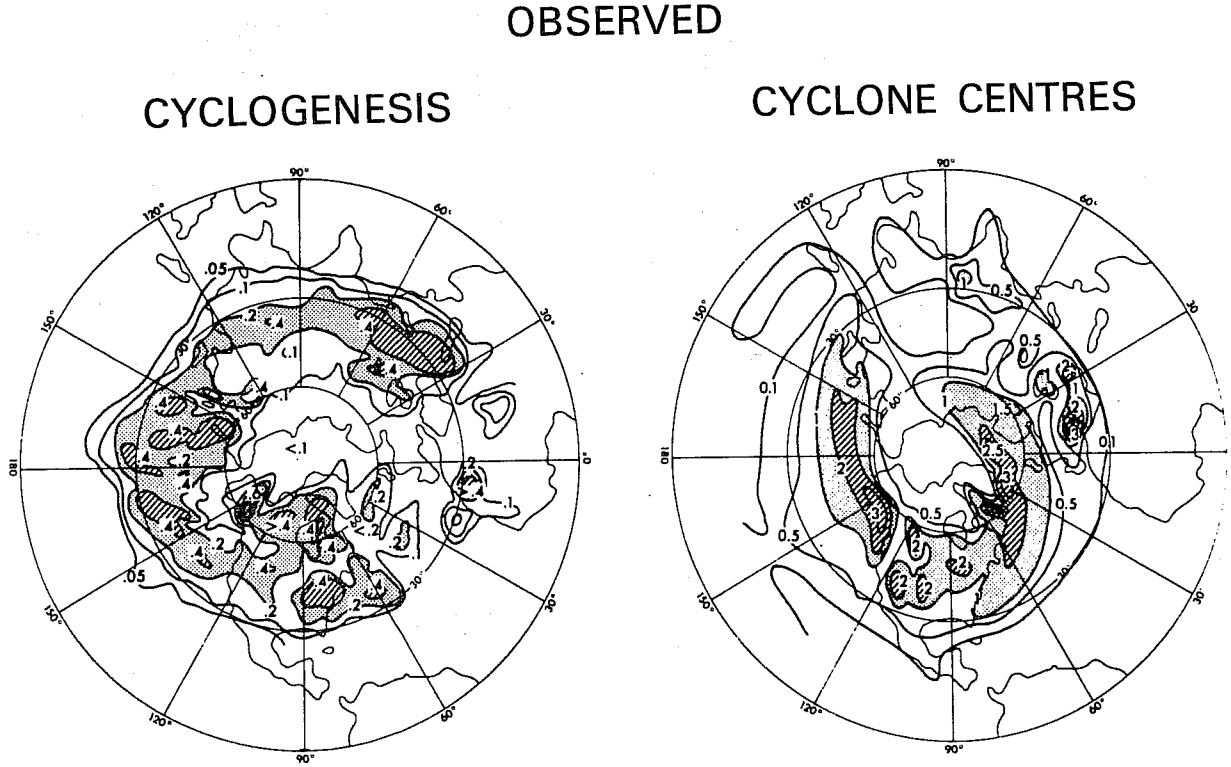

Left: Observed percentage frequency of cyclogenesis in winter. Right: observed percentage frequency of cyclone centers in winter. The frequencies refer to areas of 100,000 km² over the period 1899–1939. (After Petterssen, 1956.)

Fig. 5.12

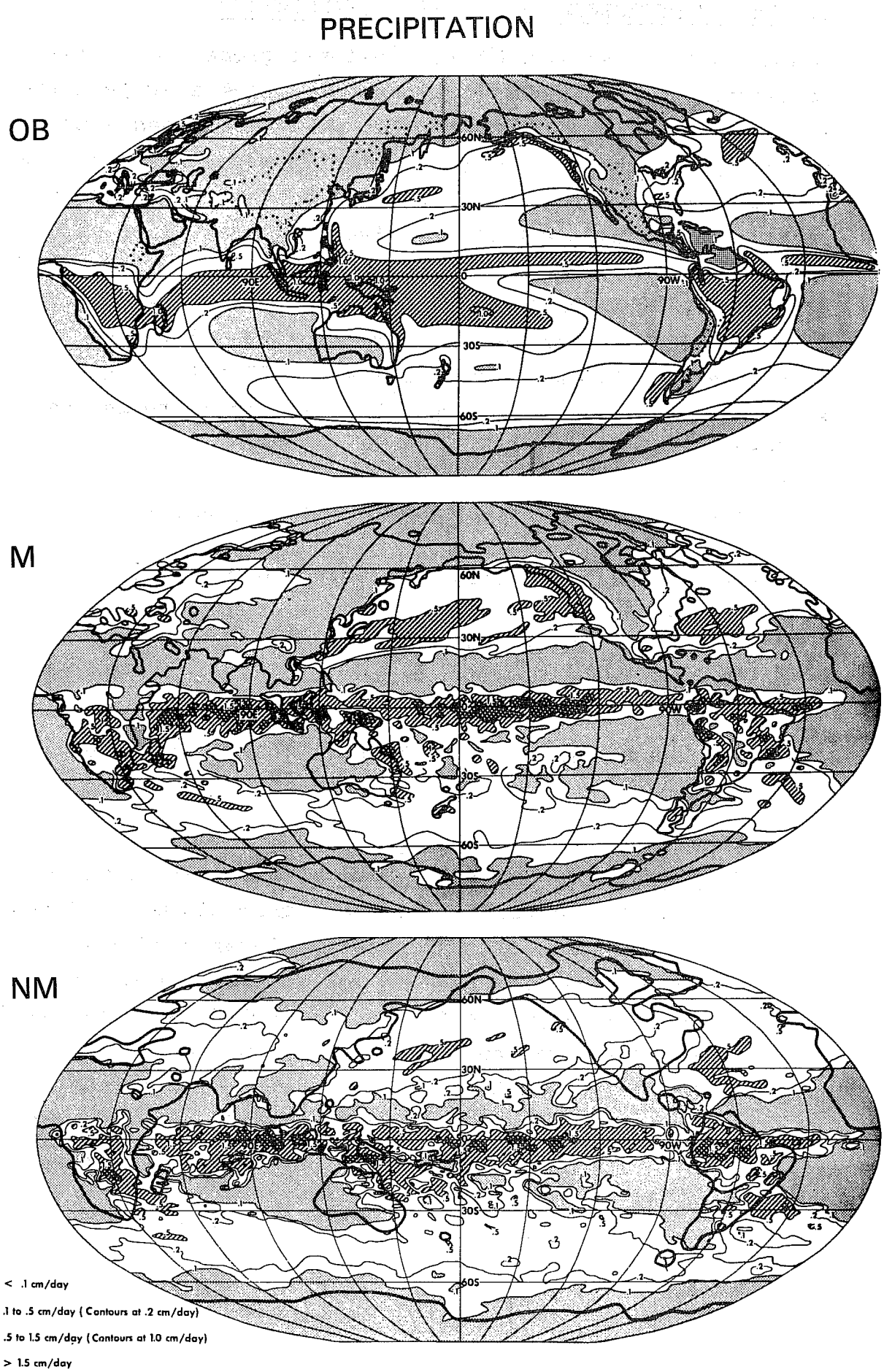

Fig.5.13 Global precipitation: observed (top), M-model (centre), NM-model (bottom). (After Manabe and Terpstra, 1974)

6. THE UK METEOROLOGICAL OFFICE EXPERIMENTS

The model used was the U.K.M.O. 5-level global GCM. The horizontal grid is a Kurihara-type grid with average horizontal resolution of about 330 km. The model uses σ as vertical coordinate. These experiments were intended as a sensitivity test to assess the value of a more realistic representation of the barrier effects of mountains.

Four control integrations of 50 days each were performed from northern hemisphere data for 1st, 12th, 13th and 14th December 1976 and three from May 1977 data. They were then repeated using orographic heights increased as follows:

All smaller-scale mountains; doubled in height.

Larger massifs [Rockies, Himalayas, Greenland]; increases limited

to { 1 km north of 63^{o}N
   { 1.5 km elsewhere

The main conclusions reported by Hills (1979) are the following:

a) Effects on the height fields (winter experiments): enhanced orography induces higher 500 mb surfaces to the north of mountains and lower surfaces downstream. (See Fig. 6.2.) In the previously reported experiments the more northerly latitude of the rises was not so evident. The overall impression is that with the enhanced orography experiment the 500 mb height field agrees rather better with observation for the years 1974-77.

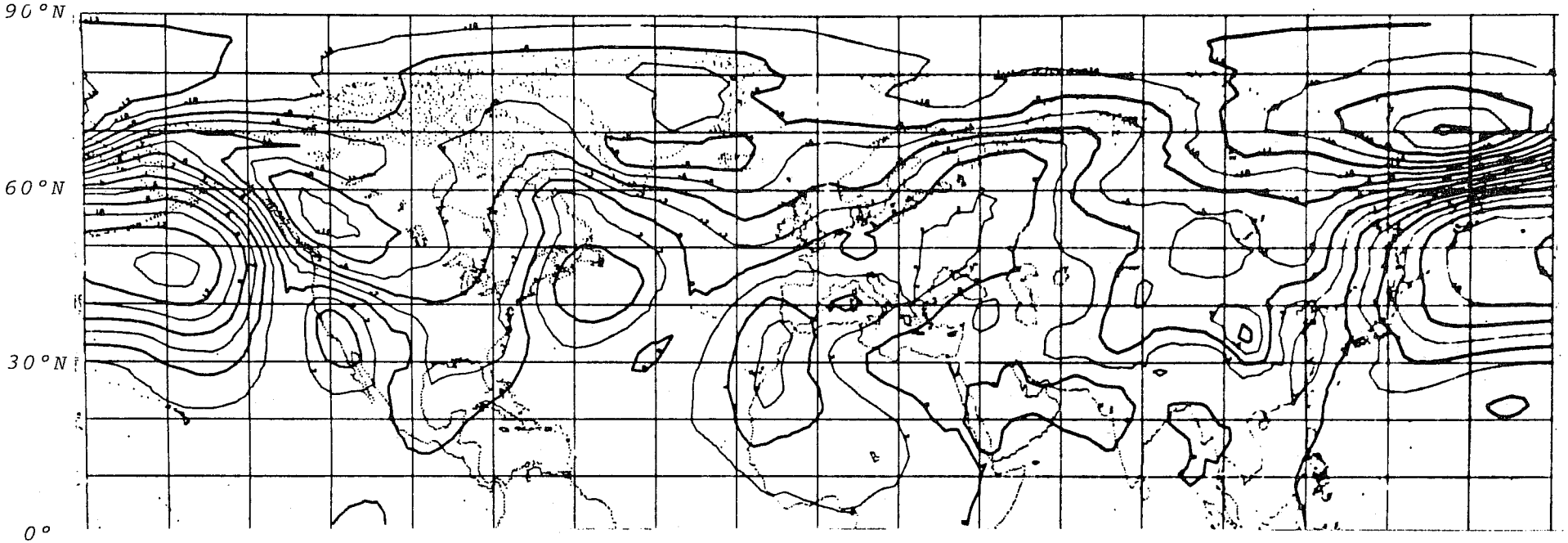

Fig. 6.1(a) Mean sea-level pressure. $\pm$ 6 mb isobars are darkened. Contour interval: 2 mb

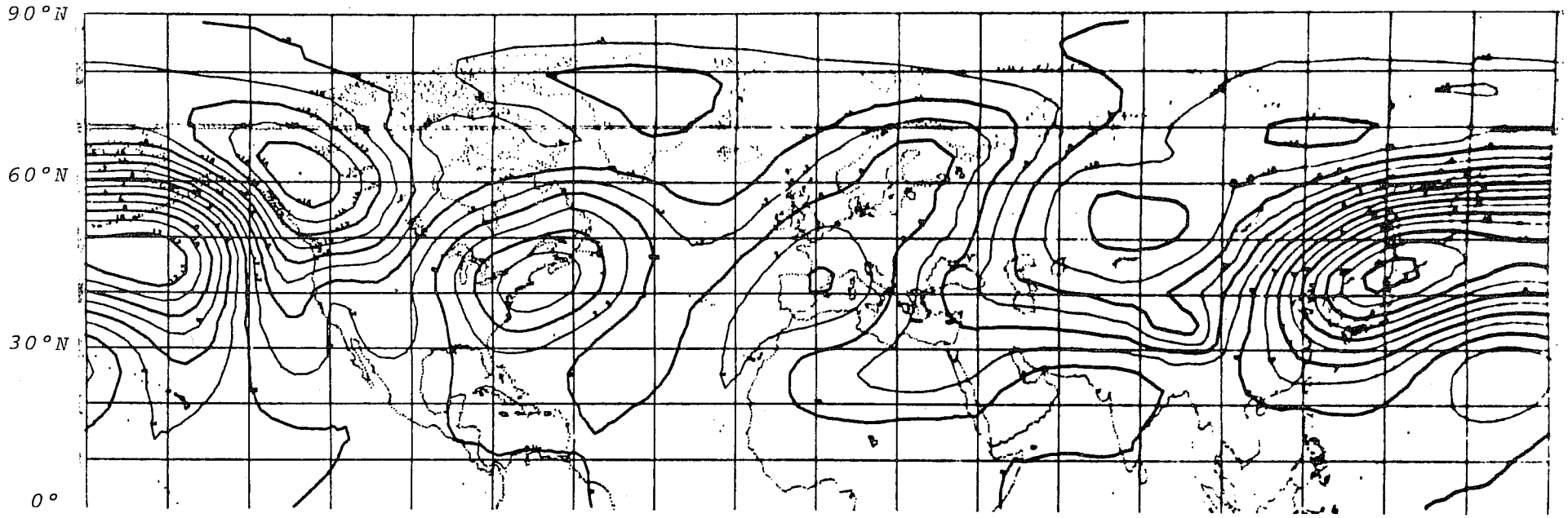

Fig. 6.1(b) 500 mb Height. $\pm$ 6 dam contours are darkened. Contour interval: 2 dam

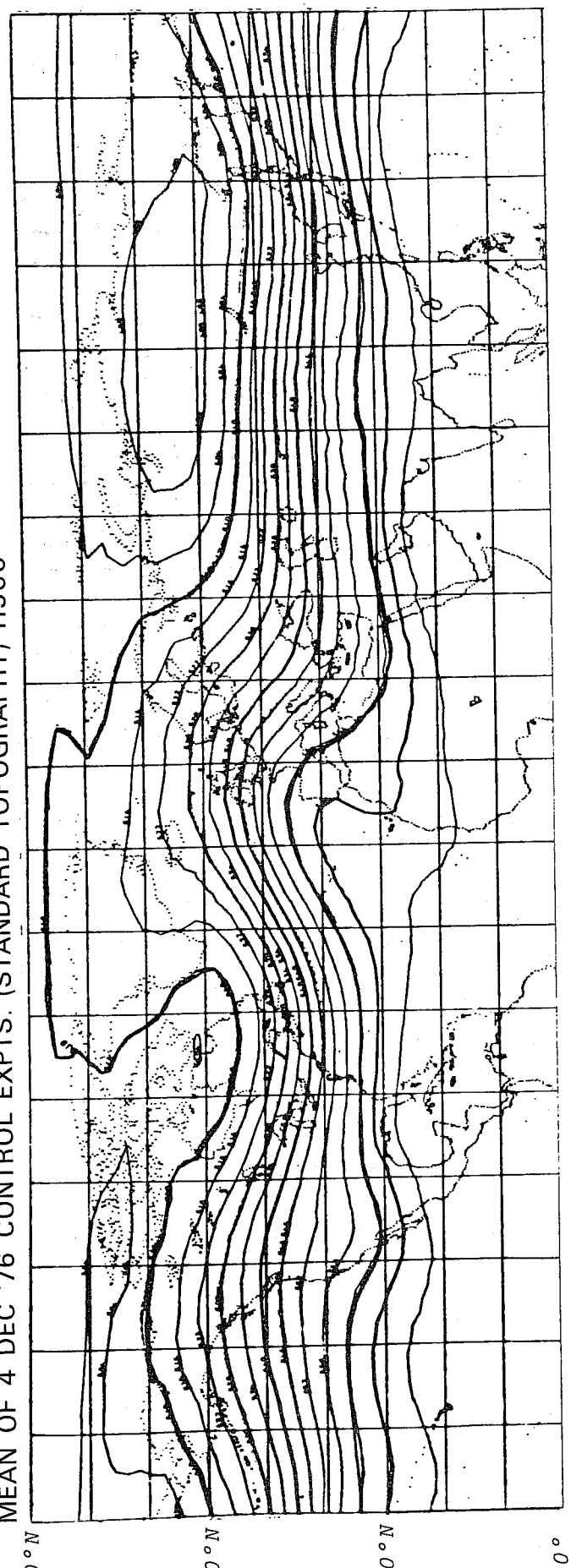

Fig. 6.2a Contour interval: 6 dam. Darkened contours: 510, 528, 546, 564 dam

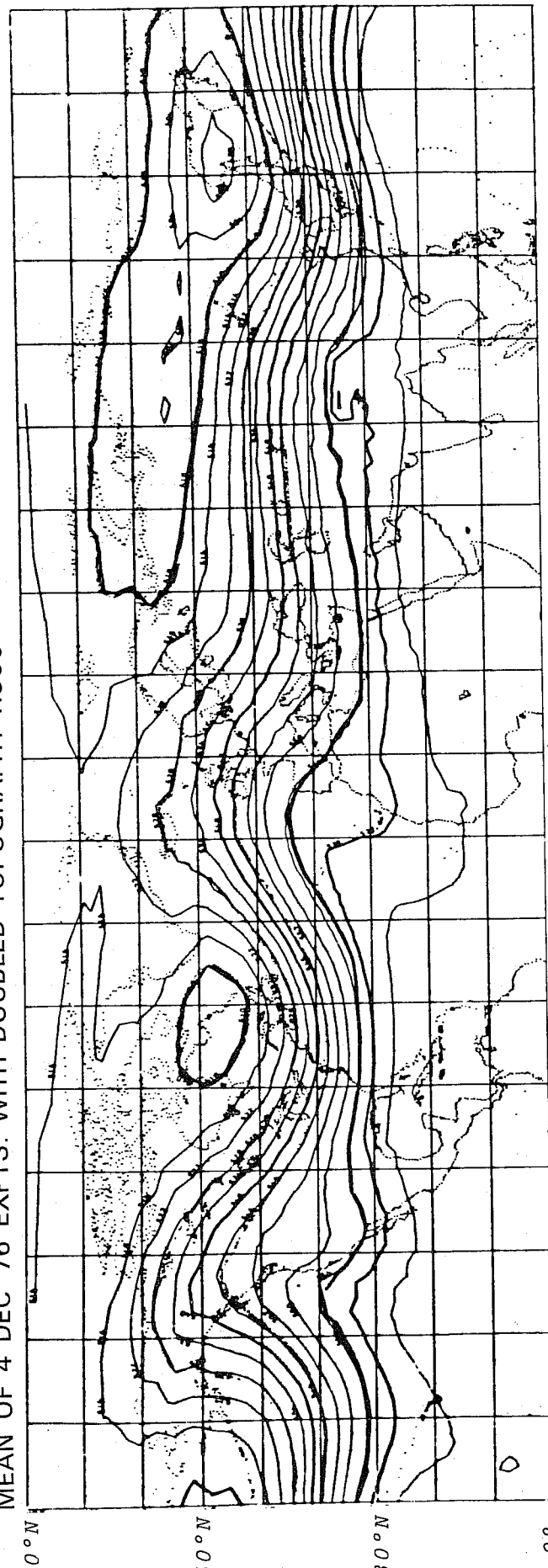

Fig. 6.2b Contour interval: 6 dam. Darkened contours: 510, 528, 546, 564 dam

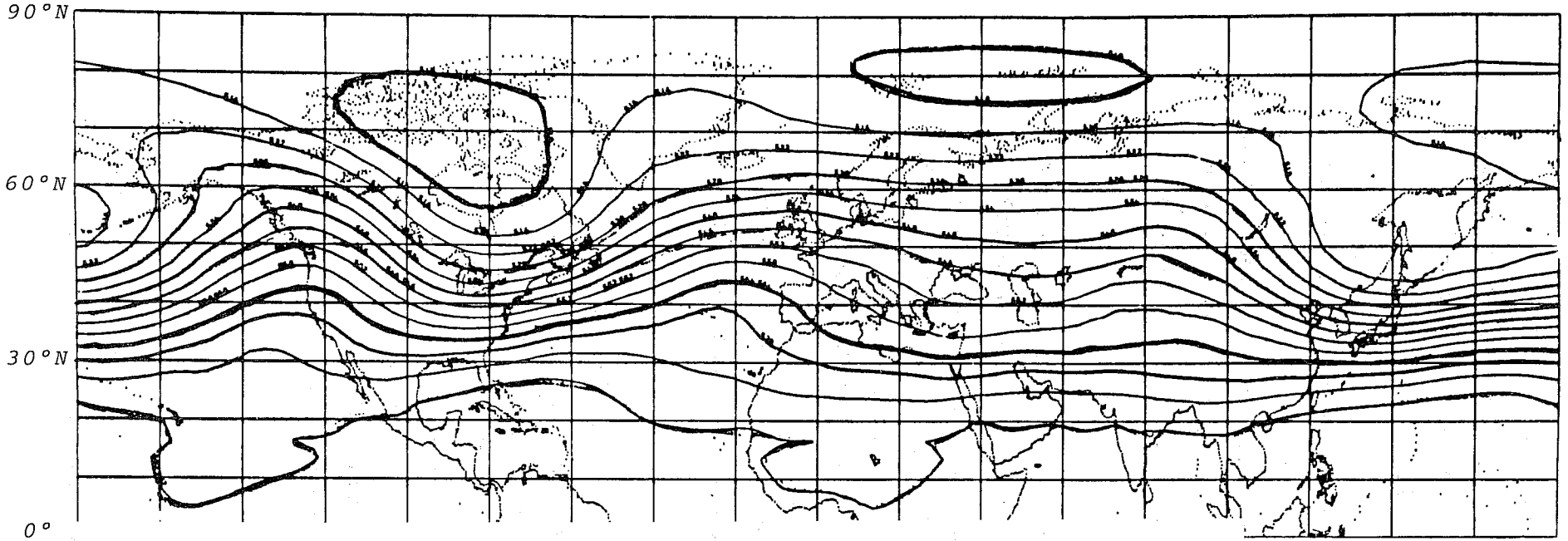

Fig. 6.2c Contour interval: 6 dam. Darkened contours: 510, 528, 546, 564 dam

DIFFERENCES OF MEANS OF 1000-500 mb THICKNESS BETWEEN STANDARD AND ENHANCED OROGRAPHY EXPERIMENTS (DECEMBER 1976)

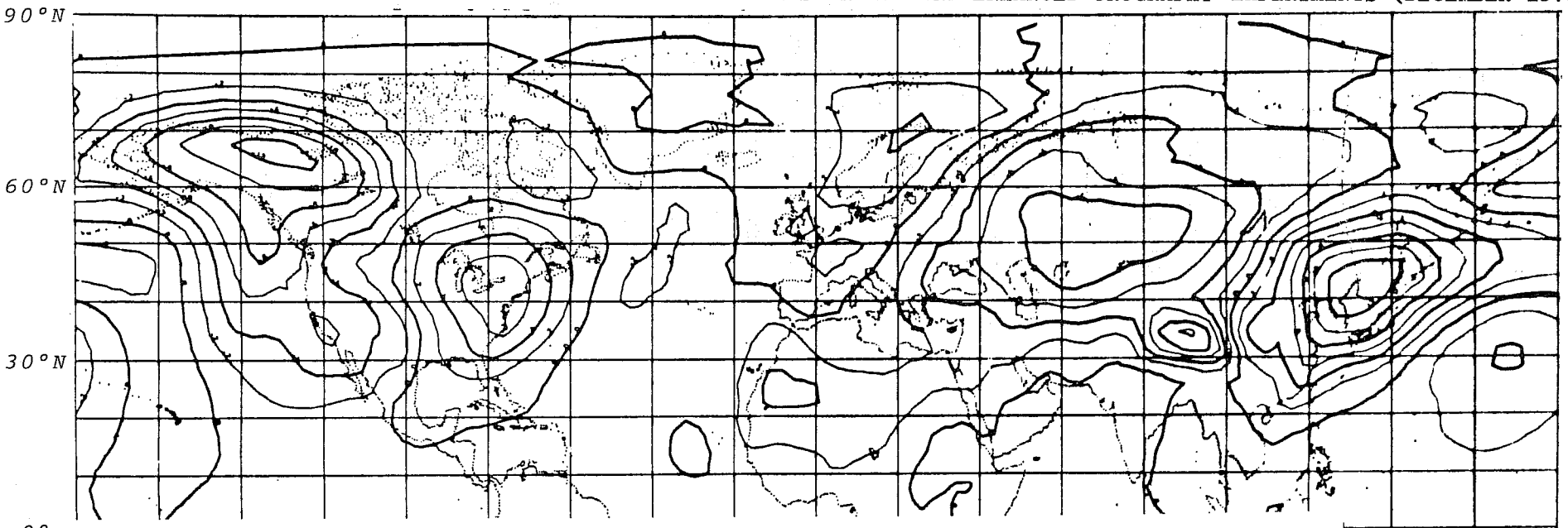

Fig. 6.3 Contour interval: 2 dam. $\pm$ 6 dam contours darkened

For example, the ridge over western North America is stronger, as is the trough over Japan. The jet to the east of Japan is increased in strength, an improvement also.

The sea level pressure increases over and to the North of the increased orography and falls downstream (Fig. 6.1). An improvement when compared with climatology is the southward movement of the Pacific subtropical ridge from 35-40°N to 25-30°N.

If we combine these changes with the changes in 500mb height we see the changes in 1000-500mb thickness shown in Fig. 6.3. There are increases (representing a warming in the lower half of the atmosphere) over and to the north of the Rockies with a maximum change of about 12 dam and increases of up to 9 dam to the north of the Himalayas. Falls of 7 dam and 13 dam occurred downstream of the Rockies and Himalayas respectively.

In a previous work (Rowntree, 1975), an earlier version of the model was run with standard orography and with no mountains at all. A cross-section of 500mb height differences along 49½°N is shown in Fig. 6.4. The three lower curves represent the effect of the mountains on the flow in these earlier experiments.
The top curve shows the results obtained by Manabe and Terpstra (1974) for comparison.

(C7-NM7) is not very like the other two, probably because the model was different and because both

experiments of the pair are different from those in the other experiment pairs. It is broadly similar to (C6-NM3), however, in having no trough near 60°E. It may be noted that the response to the orography in (C4-NM3) is to have ridges over all the mountains and in (C6-NM3) over the Rockies. In (C7-NM7), however, the ridges were well upstream of the mountains and the trough just downstream.

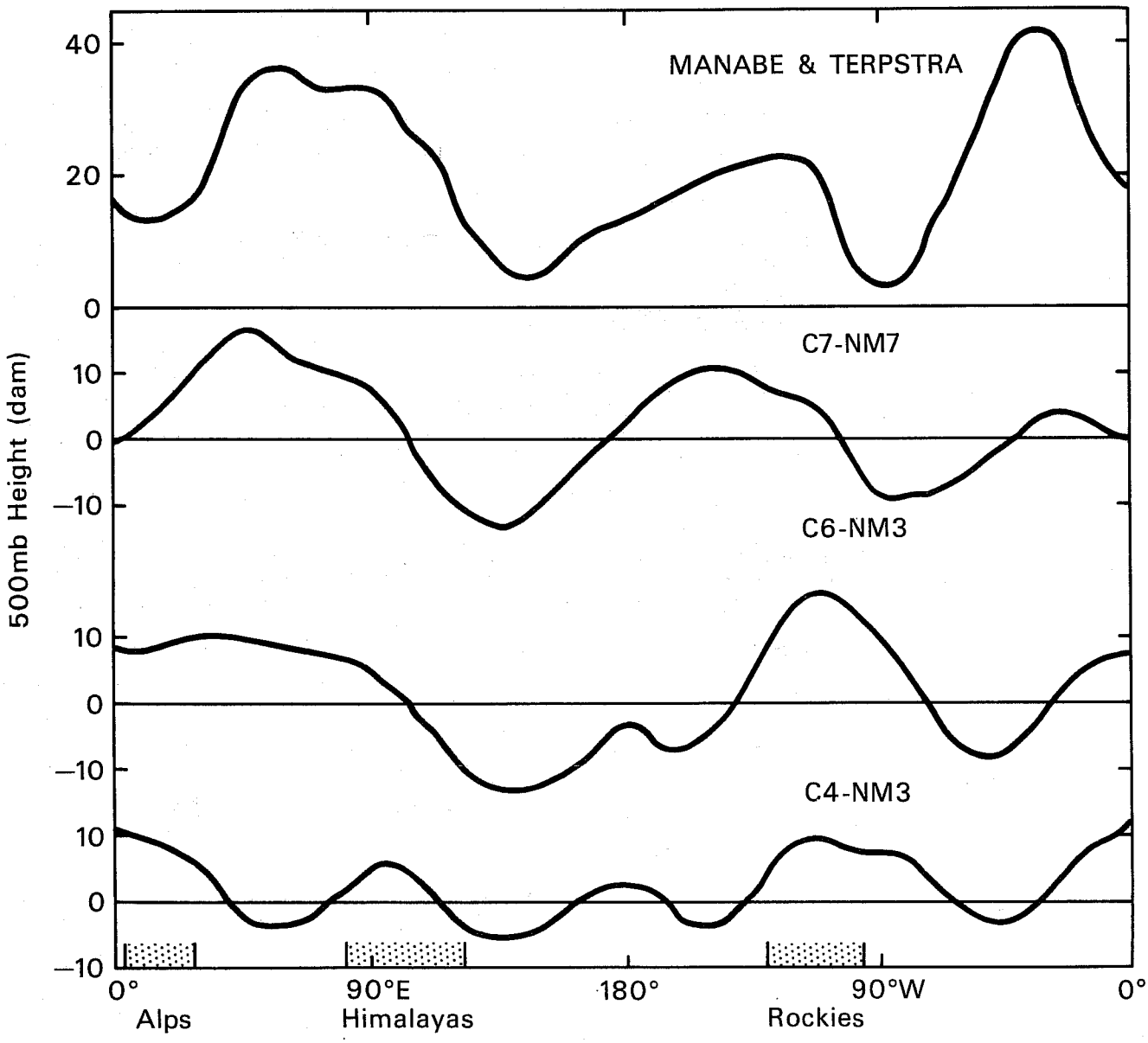

Fig.6.4 Changes in 500 mb height along $49\frac{1}{2}$ °N by inclusion of mountains. (After Rowntree, 1975).

b) Effects on the eddy kinetic energy (winter experiments): an examination of the latitudinal distribution of transient and standing eddy kinetic energy shows (Table 6.1):

(i) The hemispheric mean total eddy kinetic energy is a little increased in the enhanced orography experiments compared with the controls.

(ii) The splitting between the transient and standing energy is different in the two cases; the control experiments have more transient energy, whereas the enhanced orography experiments have more standing energy.

It appears that the increased amplitude in the orographically induced standing waves is largely at the expense of transient waves.

c) Comparison of summer integrations: the 500 mb height differences are shown in Fig. 6.5. Here the changes are predominantly increased with a regular zonal pattern.

Table 6.2 displays the eddy kinetic energy values for these experiments, and shows a rise in standing energy in the enhanced orography experiments but a rather smaller fall in transient energy, compared to the winter experiments.

Fig.6.5

DIFFERENCES OF MEANS OF H_{500} BETWEEN ENHANCED AND STANDARD OROGRAPHY EXPERIMENTS FOR SUMMER

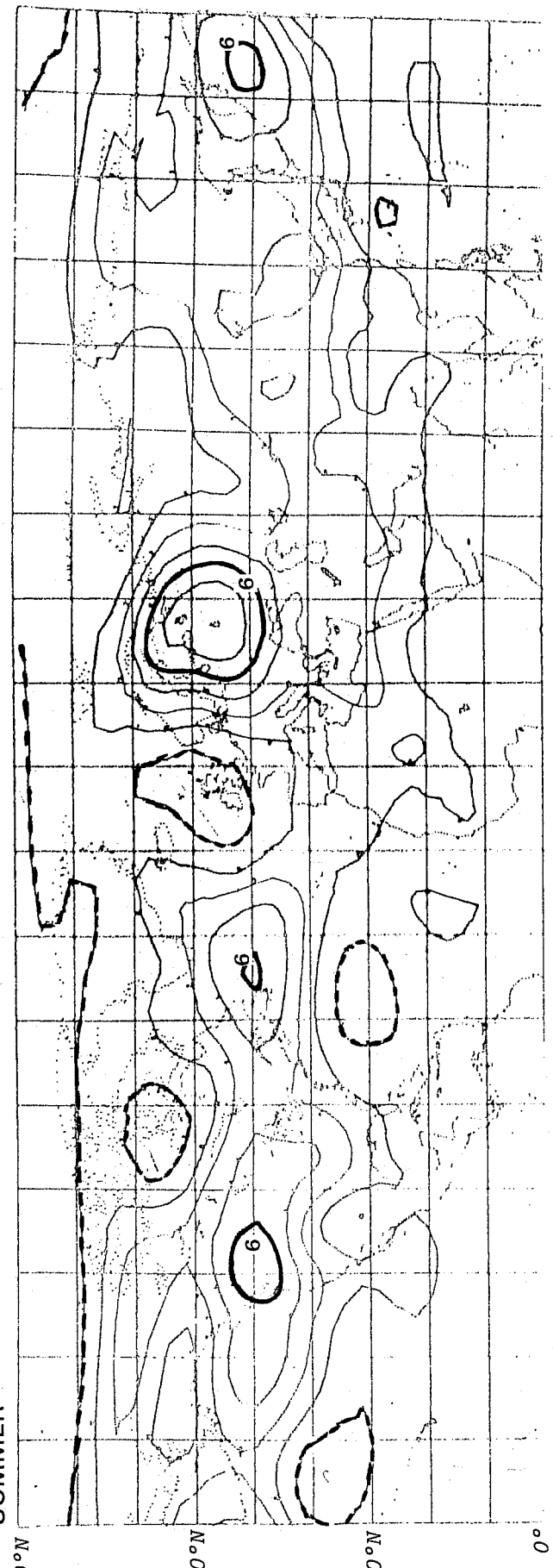

-2 dam contour is dashed. ±6 dam contours are darkened. Contour interval: 2 dam.

Hemispheric mean eddy kinetic energy ($m^2 s^{-2}$)

Experiment pair		transient	standing	total
A	Standard orography	31	20	51
	Enhanced "	28	39	67
B	Standard orography	40	29	69
	Enhanced "	26	48	74
C	Standard orography	30	30	60
	Enhanced "	29	40	69
D	Standard orography	36	31	67
	Enhanced "	27	40	67
Estimated observed values		87	17	104

Table 6.1 (After Hills, 1979)

Hemispheric mean eddy kinetic energy ($m^2 s^{-2}$)

Experiment pair		transient	standing	total
A	Standard orography	12	14	26
	Enhanced "	10	19	29
B	Standard orography	12	15	27
	Enhanced "	10	20	30
C	Standard orography	12	16	28
	Enhanced "	9	20	29
Estimated observed values		47	9	56

Table 6.2 (After Hills, 1979)

7. CONCLUSIONS

Although the presence of mountains in General Circulation Models is of paramount importance to reproduce realistically the observed patterns of motion, the relative role of orography and thermal contrast in forcing planetary waves in GCM's (as in nature) has not been clarified completely. There are some indications that would suggest that the thermal forcing is of particular importance for the tropospheric standing waves, while the orographic forcing may be more important in the upper troposphere and the stratosphere.

Linear models suggest that for vertical resolutions commonly used in prediction, or general circulation, models the upper boundary condition $\omega = 0$ at $p = 0$ may lead to serious errors in the behaviour of ultra-long waves in the troposphere. It is not at all clear that in practice the upper boundary condition generally gives rise to a problem in forecast or climate models, and some clarification of this apparent discrepancy between theory and practice is desirable.

The role of mountain complexes in influencing non-linear transfers between the various scales is not well understood. Numerical experiments indicate that orography can influence the level of transient edddy energy since weaker transients are found when standing waves are larger, but there are also indications that mountain-induced standing waves may also enhance instability, at least locally. Smaller-scale orographically force perturbations, such as for example cyclones in the lee of the Alps, have an impact on the larger scales of motion.

More sensitivity tests should be carried out, to assess the impact of more realistic topographies, both in terms of height and of steepness of large-scale mountain chains, because it is sometimes very difficult to export conclusions reached so far to models with different vertical resolution and different description of the stratospheric circulation.

References

Bolin, B., 1950: On the influence of the earth's orography on the general character of the westerlies. Tellus, 2, 184-195.

Charney, J.G., and A. Eliassen, 1949: A numerical method for predicting the perturbations of the middle latitude westerlies. Tellus, 1, 38-54.

Crutcher, H.H., and J.M. Meserve, 1970: Selected level heights, temperatures and dew points for the Northern Hemisphere. Direction of Commander, Naval Weather Service Command, USA.

Derome, J., and A. Wiin-Nielsen, 1971: The response of a middle-latitude model atmosphere to forcing by topography and stationary heat sources. Mon. Wea.Rev. 99, 564-576.

Egger, J., 1976: The linear response of a hemispheric two-level primitive equation model to forcing by tropography. Mon. Wea. Rev. 104, 351-364.

Egger, J., 1979: Orographically forced planetary flow. Proceedings of the ECMWF Workshop on "Mountains and NWP", ECMWF, Reading.

Gambo, K., 1956: The topographical effect upon the jet stream in the westerlies. J. Met.Soc. Japan, 34, 24-28.

Gilchrist, B., 1954: The seasonal phase changes of thermally produced perturbations in the westerlies. Proc. Toronto Meteor. Conf., Amer.Meteor.Soc. and Roy. Meteor.Soc. 129-131.

Grose, W.L., and B.J. Hoskins, 1979: On the influence of orography on large-scale atmospheric flow. J.Atmos.Sci. 36, 223-234.

Hills, T., 1979: Sensitivity of numerical models to mountain representation. Proceedings of the ECMWF Workshop on "Mountains and NWP", ECMWF, Reading.

Holton, J.R., 1972: An introduction to dynamic meteorology, International Geophysics Series, Vol. 16, Academic Press, New York.

Kasahara, A., 1966: The dynamical influence of orography on the large-scale motion of the atmosphere. J.Atmos.Sci., 23, 259-271.

Kasahara, A., and W.M. Washington, 1971: General circulation experiments with a six-layer NCAR model, including orography, cloudiness, and surface temperature calculations. J.Atmos.Sci., 28, 657-701.

Kasahara, A., T. Sasamori and W.M. Washington, 1973: Simulation experimental with a 12-layer stratospheric global circulation model. I. Dynamical effect of the earth's orography and thermal influence of continentality. J.Atmos.Sci., 30, 1229-1251.

Manabe, S., and T.B. Terpstra, 1974: Effects of mountains on the general circulation of the atmosphere as identified by numerical experiments. J.Atmos.Sci., 31, No.1, p.3.

Oort, A.H., and E.M. Rasmusson, 1971: Atmospheric circulation statistics. NOAA Prof. Paper 5, Govt. Printing Office, Washington, DC, 323 pp.

Petterssen, S. 1956: Weather analysis and forecasting, (Second Ed.), Vol. 1, Motion and Motion Systems. McGraw Hill Book Co., New York.

Rowntree, P.R., 1975: Thermal and orographic forcing of the northern hemisphere winter circulation in a numerical model. Met O 20 Tech. Note II/43, May 1975.

Smagorinsky, J., 1953: The dynamical influence of large-scale heat sources and sinks on the quasi-stationary mean motions of the atmosphere. Quart. J. Roy. Meteor. Soc., 79, 342-366.